Building a Functional Kinetochore: From Microtubule to Centromere

Grace Elizabeth Hamilton

A dissertation

submitted in partial fulfillment of the

requirements for the degree of

Doctor of Philosophy

University of Washington

2020

Reading Committee:

Trisha Davis, Chair

Charles Asbury

Alexey Merz

Program Authorized to Offer Degree:

Biochemistry

University of Washington

Abstract

Building a Functional Kinetochore: From Microtubule to Centromere

Grace Elizabeth Hamilton

Chair of the Supervisory Committee:
Doctor Trisha Davis
Biochemistry

Equal partitioning of duplicated chromosomes between daughter cells is a microtubule-mediated process essential to eukaryotic life. A multi-protein machine, the kinetochore, tethers chromosomes to dynamic microtubule tips, even as the tips grow and shrink through the gain and loss of subunits. The kinetochore must harness, transmit, and sense mitotic forces, as a lack of tension signals incorrect chromosome-microtubule attachment and initiates error correction mechanisms. But though the field has arrived at a "parts list" of dozens of kinetochore proteins organized into subcomplexes, the path of force transmission through these components has remained unclear. I reconstituted functional *Saccharomyces cerevisiae* kinetochore assemblies from recombinantly expressed proteins. The reconstituted kinetochores are capable of self-assembling *in vitro*, tethering centromeric nucleosomes to dynamic microtubules, and withstanding mitotically relevant forces. They reveal that two inner kinetochore protein subcomplexes, Mif2 and OA, are independently capable of transmitting force from MIND to the

centromeric nucleosome and suggest that these two pathways of outer kinetochore recruitment may be differentially regulated.

TABLE OF CONTENTS

LIST OF FIGURES

LIST OF TABLES

ACKNOWLEDGEMENTS

I have been so fortunate throughout my graduate education.

I have been lucky in my mentors, the foremost of whom is Trisha Davis. I am so grateful for her wisdom and support, for mentorship that always balances guidance and intellectual freedom. I thank Eric Muller for challenging me to think deeply about my work. I am grateful to Charles Asbury for cultivating both rigor and joy in the pursuit of science. Microtubules may grow at about the same rate as grass, but with people like Chip around to figure that fact out, it rarely feels tedious watching them. Thanks to Trisha Davis, Charles Asbury, Linda Wordeman, Justin Kollman, and Alexey Merz for serving on my thesis committee.

I have been lucky in my collaborators. Yoana Dimitrova has contributed so much to this project, both materially and intellectually. I have learned much from Luke Helgeson's patience, care, and persistence in the lab. I am beyond grateful to both of these incredible collaborators.

I have been lucky in my labmates. My thanks to Kim Fong, Luke Helgeson, Krishna Sarangapani, Emily Scarborough, and Alex Zelter in particular for patiently sharing their expertise in the lab. And to Mike Riffle and Alex Zelter for interceding with computers on my behalf.

Above all, I have been lucky in my friends. I thank Evie Henry and Rose King in particular—for making lab too much fun to leave.

DEDICATION

For Shane.

ABBREVIATIONS

bp	Base pair
CCAN	Constitutive centromere-associated network
CDE	Centromere determining element
CI	Chl4/Iml3
CIN	Chromosomal instability
CPC	Chromosomal passenger complex
Ct	C-terminal
Dam1c	Dam1 complex
DNA	Deoxyribonucleic acid
DSS	Disuccinimidyl suberate
EC	Error correction
EDTA	Ethylenediaminetetraacetic acid
FRET	Förster resonance energy transfer
GDP	Guanosine diphosphate
GFP	Green fluorescent protein
GTP	Guanosine triphosphate
IMAC	Immobilized metal affinity chromatography
IPTG	Isopropyl β-D-1-thiogalactopyranoside
Kl	*Kluyveromyces lactis*
LCMS	Liquid chromatography mass spectrometry
MBP	Maltose-binding protein
MCC	Mitotic checkpoint complex
MTOC	Microtubule organizing center
NCP	Nucleosome core particle
Ndc80c	Ndc80 complex
OA	Okp1/Ame1
PAGE	Polyacrylamide gel electrophoresis
PEG	Polyethylene glycol
PMSF	Phenylmethylsulfonyl fluoride
PTM	Post-translational modification
SAC	Spindle assembly checkpoint
Sc	*Saccharomyces cerevisiae*
SDS	Sodium dodecyl sulfate
SEC	Size exclusion chromatography
SEC-MALS	Size exclusion chromatography with multi-angle light scattering
smTIRF	Single-molecule total internal reflection fluorescence microscopy
SPB	Spindle pole body
TCEP	Tris(2-carboxyethyl)phosphine
WT	Wild-type
XL-MS	Cross-linking mass spectrometry

1 INTRODUCTION

1.1 CELL DIVISION AND THE CONSEQUENCES OF UNEQUAL GENETIC INHERITANCE

Cell division is the perpetuation of life at its most basic level. Perhaps the most crucial element of cell division is the transmission of genetic information into the next generation of cells. This necessitates faithful chromosome segregation, ensuring an equal genetic inheritance of identical chromosome sets for each daughter cell. Meiosis produces haploid gametes capable of combining and transmitting genetic information into the next generation of sexually reproducing organisms, whereas mitosis— if successful— creates genetically identical diploid daughter cells. Failure to equally partition genetic material during mitosis results in aneuploidy, defined as any number of chromosomes that is not a multiple of the haploid set.

Aneuploidy is frequently disastrous at both the cellular and organismal level; it has been observed for over a century that aneuploidy reduces the fitness of individual cells [1]. More recent work has elucidated *how* aneuploidy causes such detrimental effects: dysregulation of transcriptional networks [2,3], proteotoxic stress [4,5], and hypo-osmotic-like stress [6]. In humans, constitutional aneuploidies— those found in every cell of the body— almost always cause embryonic or perinatal lethality [7]. Fetal aneuploidy is the leading known cause of first-trimester miscarriages [8]. Those few constitutional aneuploidies that are not lethal (including trisomy 21 and sex chromosome aneuploidies) still cause severe disease [9], as do some mosaic aneuploidies [7].

And yet aneuploidy is also a hallmark of cancer. Over 90% of human solid tumors and 50% of blood cancers are aneuploid [10]. Aneuploidy is both an obvious consequence and putative cause of chromosomal instability (CIN), an elevated rate of chromosome gain or loss [11-14]. CIN generates phenotypic heterogeneity within cancer cell populations, which is proposed to increase their adaptability, metastatic potential, and resistance to chemotherapy [12,15].

Aneuploidies arise though errors in chromosome segregation, an essential process mediated by the mitotic spindle.

1.2 THE MITOTIC SPINDLE

That cells undergo massive internal reorganization before and during division was apparent to even the earlier cell biologists [16,17]. In 1882, Walter Flemming first put the name "mitosis" (from the Greek for "thread") to the stereotyped process he observed in animal cells: the condensation of threadlike chromosomes bound by an array of thinner fibers, their congression at the metaphase plate and eventual segregation to opposite poles of the dividing cell, and the re-formation of nuclei in the two resultant daughter cells [18]. The language of threadwork stuck, and the apparatus of chromosome segregation is known to this day as the mitotic spindle.

The mitotic spindle consists of microtubules nucleated by microtubule organizing centers, condensed chromosomes that must be segregated, and kinetochores, which couple microtubule dynamics to chromosome movement. The mitotic spindle also includes numerous regulatory, checkpoint, microtubule-associated, and chromatin-remodeling proteins.

1.2.1 Microtubules of the mitotic spindle

Using polarized light microscopy to observe weakly birefringent spindle fibers, Shinya Inoué pioneered our understanding of the mitotic spindle as a dynamic structure made up of labile microtubules, which tend to grow from organizing centers [19].

Centrosomes are metazoan microtubule-organizing centers (MTOCs). All fungi (save *Chytridiales* [20,21]) instead have spindle pole bodies (SPBs), acentriolar MTOCs with a tri-laminar structure that are embedded in the nuclear envelope [22]. SPBs contain the γ-tubulin small complex, which is most directly responsible for templating microtubule nucleation [23,24]. SPBs nucleate three classes of microtubules: astral microtubules, which extend towards the periphery of the cell; interpolar microtubules, which extend toward the metaphase plate but do not contact chromosomes; and kinetochore microtubules, which do capture chromosomes [25].

Microtubules are complex polymers, the most basic unit of which is the extremely stable α- and β-tubulin heterodimer. Those dimers self-assemble into polar protofilaments; the β-tubulin end is the "plus" end while the α-tubulin end is the "minus" end. A canonical microtubule is then composed of 13 such protofilaments arranged to form a hollow tube about 25 nm in diameter [26] (although other protofilament arrangements also exist [27]). These structures are usually dynamic. *In vivo*, microtubules are often capped at their minus ends by the MTOCs that nucleated them, so

they grow and shrink primarily through the gain and loss of tubulin dimers at the plus end of the polar polymer [28,29].

Building on Inoué's observation of microtubule dynamicity in living cells, Mitchison and Kirschner studied tubulin polymerization *in vitro*. In 1984, they first described "dynamic instability," the manner in which microtubules change between two states: rapid shrinkage and comparatively slow growth [29]. The transition from growth to shrinkage is known as "catastrophe," and the transition from shrinkage to growth is called "rescue." Dynamic instability results from GTP hydrolysis by tubulin [29,30]. Both α- and β-tubulin have a GDP/GTP binding site. The binding site on α-tubulin is buried and non-exchangeable; the binding site on β-tubulin is exposed and exchangeable [26]. Structural evidence suggests that hydrolysis of GTP causes compression of the exchangeable site at the interdimer interface, with a β-tubulin loop moving to fill the space formerly occupied by the γ-phosphate of GTP [31]. This transition causes an energetically unfavorable rearrangement of intermediate domain of α-tubulin, causing conformational strain that is alleviated by protofilament curling during microtubule depolymerization [31,32]. Numerous microtubule-associated proteins regulate microtubule dynamics.

The dynamicity of microtubules is essential for their mitotic function. As Inoué theorized in 1967 [33], fluctuations in microtubule length do mechanical work; using a feedback-controlled laser trap, Driver and colleagues demonstrated that protofilaments curling outward from a disassembling microtubule tip behave like springs and can generate forces of up to 16 pN [34]. *In vivo*, the disassembly of microtubule tips drives mitotic chromosome movements; kinetochores couple these two processes [35-37].

1.2.2 Centromeres and kinetochores

Kinetochores are proteinaceous structures that assemble on centromeric DNA and tether chromosomes to dynamic microtubules. Some organisms, including budding yeast and humans, have regional centromeres at the primary constrictions of chromosomes, whereas other organisms have holocentric chromosomes, with diffuse kinetochores that bind microtubules along their entire lengths [38,39]. In general, centromeric DNA is highly repetitive and AT-rich, though the size and sequence of regional centromeres vary tremendously [40,41]. The budding yeast "point" centromere, which is genetically specified by only about 125 base pairs of DNA in three

centromere-determining elements (CDEI, CDEII, and CDEIII) [42,43], is exceptional for both its diminutive size and sequence conservation [44].

Both genetic and epigenetic factors contribute to centromere identity, and their relative importance varies between organisms [41]. Budding yeast rely heavily on genetic determinants of centromere identity [41,43,45]. But in the vast majority of organisms studied thus far, centromeres are primarily specified in an epigenetic manner by the presence of a centromere-specific histone H3 variant termed CENP-A (Cse4 in budding yeast) [46,47]. CENP-A positioning is epigenetically propagated, because existing CENP-A nucleosomes template new CENP-A deposition by recruiting necessary chaperones such as HJURP (Scm3 in budding yeast) [48-51]. Indeed, in higher eukaryotes centromere inheritance appears minimally affected by DNA sequence; centromeres can migrate into neighboring regions, a phenomenon known as "centromere drift" [41,52]. Experimentally mis-targeted CENP-A can incorporate into non-centromeric chromatin (including both actively transcribed euchromatin and heterochromatin) and recruit kinetochore proteins, creating "neocentromeres" that can be transmitted mitotically for generations [53-55]. Neocentromeres also form on non-repetitive DNA without experimental manipulation— over 100 different neocentromeres have been identified in living humans [56,57]. In several such cases, the original centromeres were permanently silenced without rearrangement or deletion of formerly centromeric repeat DNA sequences [58]. In other words, in humans the presence CENP-A at a given chromosomal locus, unlike the underlying DNA sequence, is both necessary and sufficient for mitotic centromere function.

The number of microtubules associated with each kinetochore is highly variable between organisms [59]. Across 18 organisms with regional centromeres, the number of kinetochore microtubules increases in a roughly linear manner with increasing mean chromosome size (**Figure 1-1**); this may reflect the fact that centromere size tends to increase linearly with chromosome size (at least within closely related species) [60].

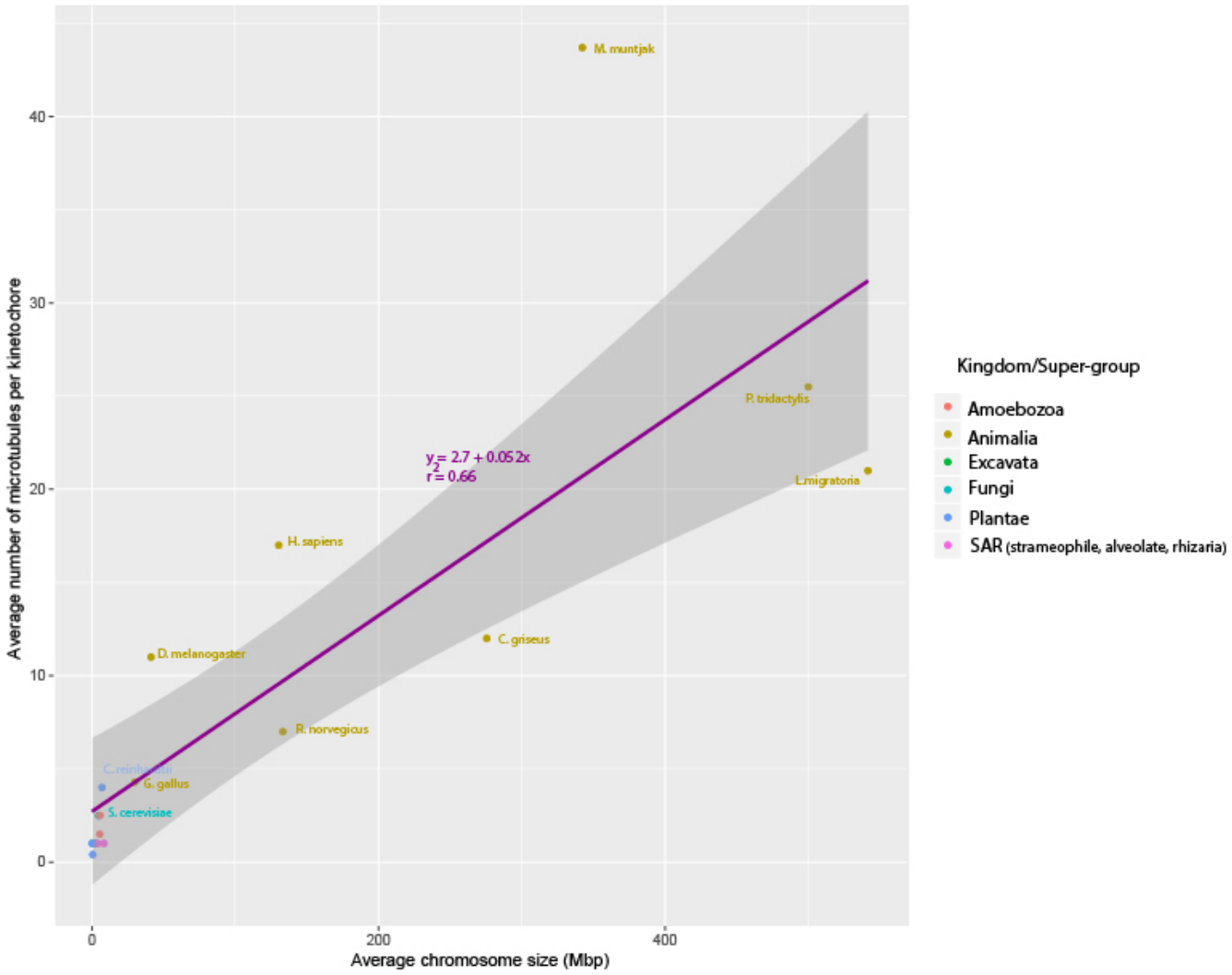

Figure 1-1. The average number of kinetochore microtubules increases linearly with mean chromosome size. Data from [59,61-66].

The paradox of absolutely essential yet poorly conserved centromeres has prompted some to view centromeric chromatin as selfish genetic elements, competing with their homologs for inclusion in gametes during asymmetrical meiotic divisions; this theory is known as "Centromere Drive" [67,68]. A corollary of this theory is that the centromere-associated proteins of the inner kinetochore should also be rapidly evolving, a prediction that appears to be borne out [69].

1.3 THE BUDDING YEAST KINETOCHORE

Saccharomyces cerevisiae has been one of the primary models for studying the kinetochore for decades, not merely because of the relative ease of performing genetic screens in yeast, but because

the budding yeast kinetochore is considerably simpler than vertebrate kinetochores in several key regards. First, while most eukaryotes have centromeric DNA regions that can span megabases [70], each *S. cerevisiae* chromosome has a single ~125 bp point centromere encompassing a single nucleosome containing the centromere-specific histone variant Cse4 [71,72]. Secondly, each budding yeast kinetochore interacts with a single microtubule during metaphase [59]. Human chromosomes, in contrast, associate with 15-25 microtubules each [61]. In addition, *S. cerevisiae* tolerates aneuploidy better than most eukaryotes [73], and thus it may be grown and studied under conditions of low segregation fidelity that would be lethal to other model systems [74]. Finally, the majority of budding yeast kinetochore proteins have well- conserved human homologs, with the notable exception of Dam1c (**Table 1**) [75].

Table 1. Proteins of the kinetochore.

S. cerevisiae	Essential to yeast ?	*H. sapiens*
Dam1c / DASH	Yes	
Ask1 (Associated with spindles and kinetochores)		
Dad1 (Duo1 and Dam1 interacting)		
Dad2 (Duo1 and Dam1 interacting)		Higher eukaryotic analog is the Ska complex
Dad3 (Duo1 and Dam1 interacting)		
Dad4 (Duo1 and Dam1 interacting)		
Dam1 (Duo1 and Mps1 interacting)		
Duo1 (Death upon overproduction)		
Hsk3 (Helper of Ask1)		
Spc19 (Spindle pole component)		
Spc34 (Spindle pole component)		
Functional analog is Dam1c		**Ska Complex**
		Ska1
		Ska2
		Ska3
Spc105c	Yes	**Knl complex**
Spc105 (Spindle component)		KNL1
Kre28 (Killer toxin resistant)		Zwint-1
Ndc80c	Yes	**Ndc80c**
Ndc80 (Nuclear division cycle)		Hec1
Nuf2 (Nuclear filamentous protein)		Nuf2
Spc24 (Spindle pole component)		Spc24
Spc25 (Spindle pole component)		Spc25
MIND	Yes	**Mis12c**

Mtw1 (Mis Twelve-like)		Mis12
Dsn1 (Dosage suppressor of *NNF1*)		Dsn1
Nnf1 (Necessary for nuclear function)		Pmf1
Nsl1 (*NNF1* synthetic lethal)		Nsl1
Cnn1c	No	CENP-TWSX
Cnn1 (Co-purified with Nnf1)		CENP-T
Wip1 (W-like Protein)		CENP-W
Mhf1 (Mph1-associated histone-fold protein)		CENP-S
Mhf2 (Mph1-associated histone-fold protein)		CENP-X
OA	Yes	CENP-QU
Okp1 (Outer kinetochore protein)		CENP-Q
Ame1 (Associated with microtubules and essential)		CENP-U
Mif2	Yes	CENP-C
Mif2 (Mitotic fidelity of chromosome transmission)		CENP-C
CI	No	CENP-NL
Chl4 (Chromosome loss)		CENP-N
Iml3 (Increased minichromosome loss)		CENP-L
NN	No	No eukaryotic homolog
Nkp1 (Non-essential kinetochore protein)		
Nkp2 (Non-essential kinetochore protein)		
CM	No	CENP-OP
Ctf19 (Chromosome transmission fidelity)		CENP-O
Mcm21 (Mini-chromosome maintenance)		CENP-P
No fungal homolog		CENP-R
CM	No	CENP-HIKM
Ctf3 (Chromosome transmission fidelity)		CENP-H
Mcm16 (Mini- chromosome maintenance)		CENP-I
Mcm22 (Mini-chromosome maintenance)		CENP-K
No fungal homolog		CENP-M
Centromeric histone	Yes	Centromeric histone
Cse4 (Chromosome segregation)		CENP-A
No fungal homolog		CENP-B
		CENP-B

Although some kinetochore proteins are unique to the kinetochore, others have homologs in vesicular transport, DNA repair, transcription, & flagellar transport [76]. Many kinetochore proteins arose through gene duplications that turned homodimers into heterodimers [76].

Budding yeast kinetochore proteins were, for the most part, first identified through genetic screens. The first human kinetochore proteins (CENP-A, CENP-B, and CENP-C) were identified as antigens recognized by the autoimmune sera of patients with CREST syndrome [46]. Biochemical analyses later revealed the organization of kinetochore proteins into evolutionarily conserved subcomplexes [77] (**Table 1**). The kinetochore may be conceptually divided into the inner kinetochore, which is centromere-associated throughout the cell cycle (and sometimes referred to as the CCAN), and the outer kinetochore, which assembles only during mitosis and mediates microtubule binding.

1.3.1 The outer kinetochore

The budding yeast outer kinetochore consists of the Spc105 complex (Spc105c), the Ndc80 complex (Ndc80c), and the Dam1 complex (Dam1c). Dam1c decamers assemble into rings, which encircle microtubules [78-80]. While no vertebrate homolog of Dam1c has been identified, it is widely accepted that the Ska complex is Dam1c's metazoan functional counterpart [81-83]. Ndc80c is a tetramer made up of coiled coils in a conformationally flexible, elongated rod, with functional globular domains at either end [84,85]. Binding of the MIND complex to one of these globular domains alleviates autoinhibition within Ndc80c, opposing a tighly bent confomration that would otherwise inhibit the other globular domain's interaction with microtubules [86]. Previous studies using purified proteins have concluded that Ndc80c and Dam1c, while both capable of binding microtubules individually, cooperate to bind dynamic microtubule plus ends [87-93], that this process is regulated by Ipl1[89,90,94-97], and that Ndc80c transmits force to MIND [98-100].

1.3.2 MIND

The MIND complex binds Ndc80c, bridging the inner and outer kinetochore. Both the budding yeast *Kluyveromycces lactis* (*K. lactis*) [19] and human [20] MIND structures have been published, revealing a conserved Y-shaped tetramer in which the N-termini of all four substituents are oriented towards the inner kinetochore. The N-termini of Nnf1 and Mtw1 comprise "head I" of the Y; the N-termini of Dsn1 and Nsl1 comprise "head II." Inner kinetochore proteins Ame1 and Mif2 both bind to head I, while head II serves a regulatory function auto-inhibiting this interaction unless phosphorylated by Ipl1$^{\text{Aurora B kinase}}$ [19]. The same mechanism regulates the

MIND-Mif2 interaction in humans [20], indicating that the interface between MIND and the inner kinetochore is organized and regulated by a conserved mechanism.

1.3.3 Okp1/Ame1 (OA)

Two of only three essential components of the budding yeast inner kinetochore, Okp1 and Ame1 (OA) interact with many inner kinetochore proteins [101]. Although OA was once considered part of the canonical COMA complex (Ctf19, Okp1, Mcm21, and Ame1) [102], recent structural work suggests that OA is more intimately associated with the inessential proteins Nkp1 and Nkp2 [103]. The structure of this newborn "NANO" complex bears a striking similarity to the Y-shaped architecture of MIND [76,103]. Although not part of the same subcomplex as OA, Ctf19 and Mcm21 do rely on binding to OA for kinetochore recruitment; they in turn recruit numerous downstream CCAN components [101,104-106].

OA binds MIND through the extreme N-terminus of Ame1 (residues 1-20) [99,107,108] and binds the N-terminus of Cse4 though the Okp1 core domain (residues 166–211) [109,110]. Both of these interactions are regulated by post-translational modifications (PTMs) [99,110]. Purified OA also binds both centromeric and non-centromeric DNA [107].

Human $OA^{CENP\text{-}QU}$ is reported to bind microtubules, suggesting that, unlike fungal OA, it might function in the outer kinetochore [111]. In budding yeast, OA and Mif2 sit at the top of published CCAN recruitment hierarchies [104,105].

1.3.4 Mif2

Identified and named for its role ensuring mitotic fidelity [112], Mif2 is the third essential component of the inner kinetochore. Both overexpression and depletion of Mif2 result in chromosome missegregation and cell cycle arrest [113].

Mif2 dimerizes through a C-terminal cupin fold, which is the only major region of the large protein that has been elucidated structurally [114,115]. (A much smaller region, 16 residues of the conserved CENP-C domain of *Rattus norvegicus* $Mif2^{CENP\text{-}C}$ has been crystallized in complex with a recombinant nucleosome. It recognizes hydrophobic residues at the C-terminus of human $Cse4^{CENP\text{-}A}$ [116].)

Mif2 is involved in recruiting a number of other inner and outer kinetochore components to the centromere [104,114]. A single Mif2 dimer binds the AT-rich CDEIII region of each yeast

point centromere though an ~10 bp "AT-hook" motif located at residues 256-549 [114,117]. Purified Mif2 binds centromeric nucleosomes, specifically recognizing both Cse4 and centromeric DNA [118]. Mif2 co-purifies with MIND and forms a defined complex; this conserved interaction is mediated by the extreme N-terminus of Mif2 [99,107,108].

The essential functions of Mif2 appear to be broadly conserved. Human Mif2^{CENP-C} directly binds the C-terminus of Cse4^{CENP-A} in nucleosomes [119,120], and in *Xenopus* egg extracts Mif2^{CENP-C} is essential for *de novo* Cse4^{CENP-A} deposition during mitosis [121]. Intriguingly, Mif2^{CENP-C} is the only CCAN component that has been identified in the highly divergent, simplified kinetochores of *D. melanogaster* and *C. elegans* [122].

1.3.5 Inessential inner kinetochore protein subcomplexes

Except for OA and Mif2, all components of the budding yeast inner kinetochore are inessential. Although most have human homologs, many CCAN proteins have been lost in other lineages over evolutionary time [69,123].

Chl4/Iml3 (CI) is an inner kinetochore protein complex of particular interest because, like Mif2, it binds directly and specifically to centromeric, Cse4-containing nucleosomes [23-25]. Human Chl4^{CENP-N} recognizes centromeric nucleosomes through specific interactions with charged residues in the L1 loop of Cse4^{CENP-A} that are absent from histone H3; this interaction is strengthened through electrostatic interactions between basic amino acids on Chl4^{CENP-N} and the phosphate backbone of DNA [27,28]. A recent structure captured the basic groove of Chl4 binding the unwrapped DNA at one end of a centromeric nucleosome [124]. Yet CI requires OA and Ctf19/Mcm21 for recruitment to the kinetochore [104,105].

Cnn1/Wip1 is of interest as a potential mediator of outer kinetochore recruitment. Biochemical studies have demonstrated that human Cnn1^{CENP-T} recruits up to three Ndc80c (directly and through MIND^{Mis12c}) [65]. Using a novel kinetochore assembly assay to examine recruitment dependencies, Lang, Barber, and Biggins further elucidated this pathway in budding yeast; they determined that Cnn1 is downstream of most inner kinetochore proteins save Mif2 [31]. Because both Mif2 and Cnn1 can recruit Ndc80c (either directly or through MIND), Lang and colleagues conclude that they represent two distinct pathways of outer kinetochore recruitment [31].

1.3.6 Centromeric nucleosomes

A H3 histone variant epigenetically confers centromere identity in almost all species studied thus far (with the possible exception of kinetoplastids and certain holocentric insects) [125-128]. This histone, Cse4 in budding yeast, is 46% identical to canonical H3, but has a much longer N-terminal tail [47].

While there is consensus that a single Cse4-containing nucleosome is present at each budding yeast centromere (although there is also evidence for additional Cse4-containing nucleosomes randomly positioned within the flanking pericentric chromatin [129]), the exact composition of that centromere is a point of controversy [47,130-134]. A widely accepted model is the most conventional one: an octameric nucleosome containing two copies each of Cse4, H2A, H2B, and H4 wrapped with DNA in a left-handed manner [134-136]. But evidence has also been published supporting "hemisome [133]," "tetrasome [137]," "hexasome [138]," and "trisome [139]" models; in 2011, Black and Cleveland proposed to reconcile this confusion with a model in which centromeric nucleosomes mature throughout the cell cycle [140]. In this model, $Cse4^{CENP-A}$ occupies a pre-nucleosomal trisome or hexasome during $Scm3^{HJURP}$-mediated deposition, a tetrasomal intermediate prior to H2A:H2B addition, and a standard octameric nucleosome for the rest of the cell cycle [140]. Within a year, biophysical evidence of centromeric nucleosomes undergoing cell cycle-coupled structural transitions in both yeast and humans was published [141,142]. However, in 2017 the Cleveland Lab — early proponents of centromeric nucleosome maturation — mapped all of the sequences bound by human $Cse4^{CENP-A}$ onto individual α-satellite arrays in centromere reference models and concluded that $Cse4^{CENP-A}$ centromeric chromatin is made up of conventional octameric nucleosomes throughout the cell cycle, a conclusion supported by their biochemical, hydrodynamic, and solid-state nanopore analyses [143].

Numerous PTMs to Cse4 have been reported. Both methylation of R37 and acetylation of K49 inhibit the interaction between Cse4 and Okp1 [110]. Cse4 is also phosphorylated at several sites by mitotic kinases Cdc5 and Ipl1, and four of these phosphorylation sites exhibit a genetic interaction with Ame1 and Okp1 [144,145].

1.4 FORCE AND TENSION IN MITOSIS

The ability of the kinetochore to withstand, transmit, and sense tension force is integral to its biological function.

1.4.1 Quantification of mitotic forces in vivo

Published estimates of the forces exerted upon kinetochore-microtubule attachments in various organisms span orders of magnitude (**Table 2**). The earliest measurement comes from Nicklas, who calculated the tension force experienced by chromosomes in meiotic grasshopper spermatocytes based on chromosome elongation [146].

More recently, work from the Bloom Lab has elucidated several aspects of mitotic tension in budding yeast. Using *in vivo* fluorescence microscopy, Joglekar and colleagues demonstrated that the kinetochore is elongated by tension during metaphase and shortens when tension is lost in anaphase, mainly due to shortening of Ndc80c [147]. Mitotic forces strong enough to break dicentric chromosomes are generated before anaphase onset [148]. By visualizing the relaxation dynamics of the broken dicentric chromosomes, Fisher and colleagues calculated that the chromosomes had been under a tension force of about 0.2 pN [149].

Also working in *S. cerevisiae*, Chacon and colleagues quantified pericentromeric tension at metaphase at 4-6 pN *in vivo* by tracking thermally driven movements of pericentromeric fluorescent tags, which were used to quantify pericentromeric stiffness, from which tension was calculated using Hooke's Law [150].

While precise measurements and estimates of the force experienced by kinetochores vary (**Table 2**), there is consensus that the kinetochore withstands physiologically significant levels of tension force on the scale of pN. It is worth noting that this is considerably more force than is theoretically required to move even a relatively large chromosome through a viscous cellular environment, for which only an estimated 0.1 pN is necessary [146].

Table 2. Selected measurements of force at kinetochores.

Force per microtubule (pN)	Organism	Technique	Reference
0.1 - 100	*Melanoplus* sp.	Micromanipulation	[146]
1 - 74	*T. granulosa*	DIC microscopy and digital image processing	[151]
0.2	*S. cerevisiae*	*in vivo* chromatin relaxation dynamics following the breakage of a dicentric chromosome subjected to mitotic forces	[149]
12 - 62	*D. melanogaster*	FRET force senor in $Mif2^{CENP-C}$; talin/vinculin-based force sensor	[152]
5 - 10	*S. cerevisiae*	Simulation based on data from a FRET biosensor in Ndc80c	[153]
4 - 6	*S. cerevisiae*	Imaging-based quantification of pericentromere stiffness and stretch	[150]

The kinetochore is not merely a simple force transmitter. The kinetochore is the primary site where force is produced to power chromosome movement [35]. It is also a complex force coupler, meaning that load is non-linearly distributed among the protein complexes of the kinetochore. Suzuki and colleagues demonstrated this using a FRET tension sensor in Ndc80c; inter-kinetochore distance (centromere stretch) occurred despite a lack of tension at the biosensor [153].

1.4.2 Tension as a signal of correct attachment

Two major regulatory systems ensure that mitosis does not proceed when the mitotic spindle is improperly organized. Several types of erroneous kinetochore-microtubule attachment must be recognized (**Figure 1-2**). Because chromosome capture by microtubules is a stochastic process, one kinetochore on a given chromosome will usually be contacted before the other, creating a transient monotelic attachment that, if it persists, will trigger mitotic delay [154,155]. Syntelic attachments, in which sister kinetochores are contacted by microtubules emanating from the same pole, do not generate tension. Bioriented chromosomes may represent proper, amphitelic attachments, or— in organisms whose kinetochores can bind multiple microtubules— they may

represent erroneous, merotelic attachments. Merotelic attachments are particularly dangerous and a major source of aneuploidy in cultured mammalian cells, likely because their kinetochores are both attached and under tension [156,157].

The error correction mechanism recognizes kinetochore-microtubule attachments that are not under tension, while the spindle assembly checkpoint recognizes unattached kinetochores [158]. When functioning correctly, these two systems promote accurate chromosome segregation during mitosis.

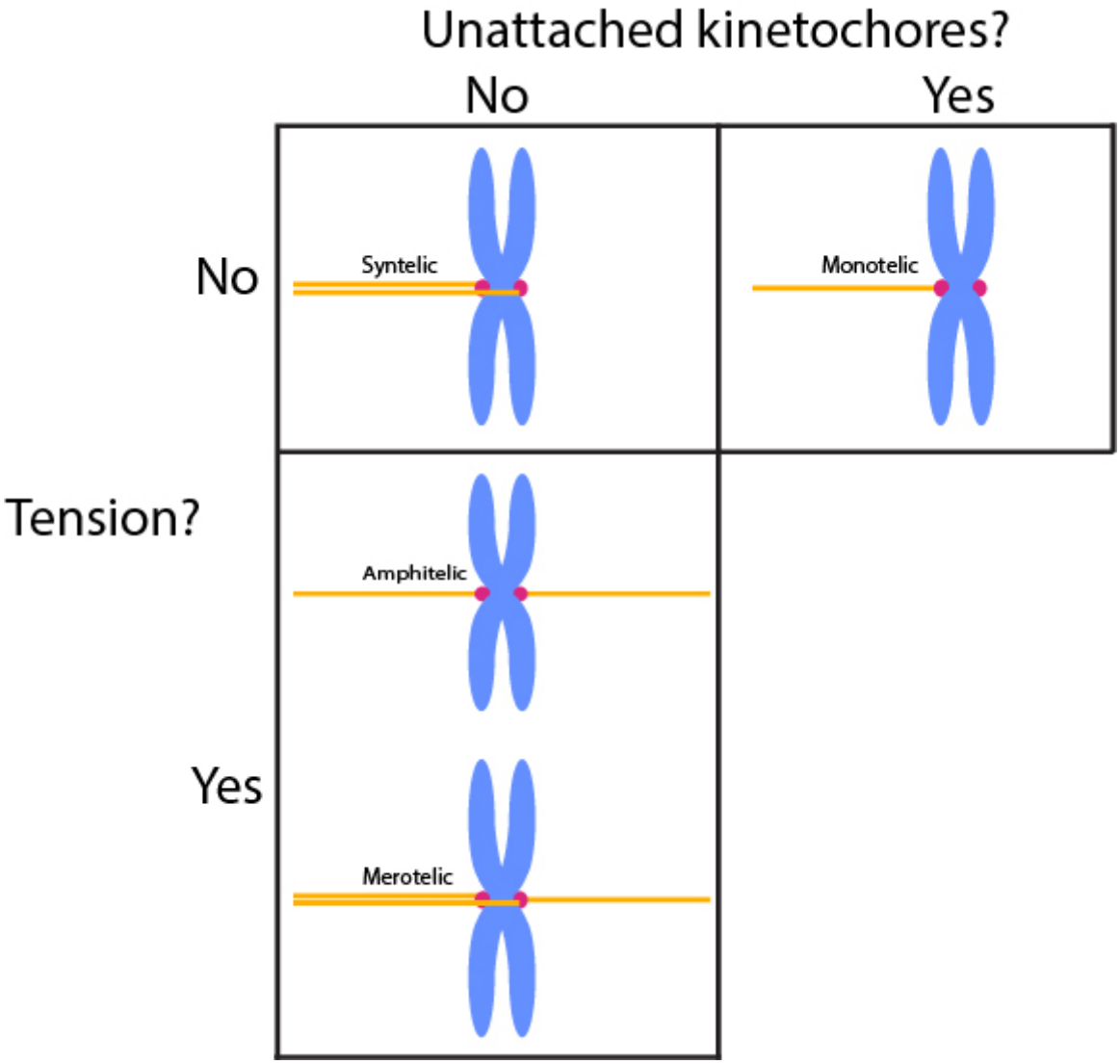

Figure 1-2. Types of kinetochore-microtubule attachment. Chromosomes are shown in **blue**, microtubules in **yellow**, and kinetochores in **red**. Error correction (EC)

Tension is the fundamental signal of chromosome biorientation, without which an error correction (EC) mechanism arrests the cell cycle until biorientation is achieved. This has been

known since the seminal work of Bruce Nicklas using grasshopper spermatocytes; Nicklas used a glass microneedle to artificially apply tension to maloriented chromosomes, which would then remain stably maloriented for hours, unlike relaxed chromosomes, which reoriented in minutes [159].

In the absence of EC, cells can leave mitosis early, with unattached or improperly attached chromosomes that may then be mis-segregated [160]. Correct attachments put kinetochores under tension, because cohesin holds sister chromatids together, while microtubules emanating from opposite poles of the cell pull them apart [161].

The mitotic kinase Ipl1, like its mammalian homolog Aurora B kinase, is necessary to correct incorrectly attached kinetochores [162,163]. Phosphorylation by Ipl1 decreases the affinity of outer kinetochore components for microtubules [97,161], causing detachment of aberrantly attached kinetochores, thus activating the SAC [163].

1.4.2.2 Spindle assembly checkpoint (SAC)

The SAC detects unattached kinetochores; a single unattached kinetochore is sufficient to activate the SAC and delay anaphase [154,164,165]. But the SAC response is not a binary on/off switch; it can be activated to different levels, which then determine the length of mitotic delay [166].

The conserved mitotic kinase Mps1 localizes to unattached kinetochores and phosphorylates both kinetochore and SAC proteins [167,168]. This initiates a signaling cascade that leads to the formation of the mitotic checkpoint complex (MCC), which inhibits formation of the anaphase-promoting complex, a ubiquitin ligase that would otherwise target Securin (which sequesters Separase, preventing it from degrading cohesin) and Cyclin B from ubiquitin-mediated proteolysis [169,170]. Thus, mitotic checkpoint proteins prevent sister chromatid separation and mitotic progression until every single kinetochore is attached. This delay gives microtubules a chance to contact the unattached kinetochore and achieve chromosome biorientation, at which point the SAC is silenced through the activity of PP1, which dephosphorylates certain substrates of the SAC kinase Bub1 [171-174]. Whether or not Ipl1 is directly involved in the SAC is controversial [158,162,175,176].

Many tumor cells have an abnormal SAC [177-179]. In healthy cells, tension is the signal of correct attachment without which EC creates unattached kinetochores, activating the SAC. Thus, there is considerable interest in how tension is transmitted through the kinetochore.

1.4.3 Optical trap-based quantification of kinetochore load-bearing ability in vitro

Invented by Arthur Ashkin in 1970, the optical trap (also known as optical tweezers) uses the radiation pressure of focused lasers to manipulate and monitor the positions of micron-scale objects with sub-nanometer precision [180]. Depending on the stiffness of the trap, forces of approximately 1-200 pN may be exerted and measured [181]. The optical trap has been used to study numerous biological systems, including motor proteins [182-185], transcriptional machinery [186], DNA [187,188], and— of course— the mitotic spindle.

Optical trap-based studies of the kinetochore may be divided into two classes: those that rely on recombinantly expressed and purified proteins and those that use kinetochore particles isolated directly from cell extracts. Akiyoshi and colleagues affinity-purified kinetochore particles from budding yeast extracts using an epitope tag on the central MIND complex and found that they could bind dynamic microtubule plus ends with a mean rupture force of 9.1 ± 0.2 pN [189]. Purified kinetochore particles also exhibited longer lifetimes of attachment to microtubules under moderate force than they did under low force, demonstrating that tension directly stabilizes kinetochore-microtubule attachments [189]. Using purified kinetochore particles, Ipl1-mediated kinetochore detachment has recently been reconstituted using an *in vitro* optical trap-based flow assay, demonstrating that tension on kinetochores is insufficient to prevent Ipl1-triggered detachment from microtubules [190]. Because tension on kinetochore proteins themselves is apparently *not* the cue, the means by which kinetochores do sense tension remains unclear. It should be noted that, in these experiments, force was only being transmitted through the outer kinetochore.

The outer kinetochore has also been the focus of optical trap studies using reconstituted protein subcomplexes. Studies monitoring the interactions between microbeads coated in purified Dam1c and dynamic microtubules revealed that the decameric complex is a robust microtubule coupler and does not require ring formation for dynamic microtubule attachment, although oligomerization does improve microtubule coupling [87,191,192]. Similar studies with Ndc80c revealed that it, too, is a competent microtubule coupler (though only when multiple copies are

present [88,92]), and that cooperation between Ndc80c and Dam1c enhances microtubule coupling and is regulated by Ipl1 [88,90,193]. Adhering MIND to microbeads and including Ndc80c and Dam1c in solution in optical trap assays revealed that force is transmitted from Ndc80c to MIND and that the MIND/Ndc80c interface is mechanically strong relative to the Ndc80c/microtubule interface [98]. Relatively little is known about force transmission through the inner kinetochore.

As kinetochore reconstitution efforts have finally reached the inner kinetochore [98,103,111,194], the stage is set to explore force transmission to the centromere using the same biophysical techniques that have elucidated microtubule coupling by the outer kinetochore.

2 RECONSTITUTION OF A FUNCTIONAL KINETOCHORE

2.1 INTRODUCTION

Chromosome segregation is a complex imperative faced by all eukaryotes, as failure to accurately distribute genetic material to daughter cells in mitosis and meiosis causes potentially lethal aneuploidy [14,156,195]. Eukaryotic cells rely on a network of protein complexes (**Table 1** and **Figure 2-2A**) to tether centromeres to the dynamic spindle microtubules that pull them to opposite poles of the dividing cell [196].

This network, the kinetochore, mediates the vital process of chromosome segregation by coupling microtubule dynamics to chromosome movement. The inner kinetochore binds the centromere; the outer kinetochore binds microtubules. A massive molecular machine, the kinetochore must harness the force of depolymerizing microtubules, transmit this force to the centromere, and sense aberrant attachments that fail to generate force. The kinetochore also serves as a regulatory hub for detection of unattached kinetochores and destabilization of improper kinetochore-microtubule attachments [197]. Tension is the signal of correct attachment (i.e. biorientation) [198], and it directly stabilizes kinetochore-microtubule connections [189]. But which of the myriad kinetochore proteins actually take part in force transmission and how much tension the kinetochore is under are unresolved.

Estimates of mitotic forces experienced by kinetochores *in vivo* span orders of magnitude [146,149,152]. For budding yeast kinetochores, estimates range from 0.2 to 16 pN [149,150,153,199]. Purified kinetochore particles isolated from budding yeast couple to microtubule plus ends with an average rupture strength in this range: 9.1 pN [97,189,200].

Previous studies using purified proteins have concluded that (1) Ndc80c and Dam1c, while both capable of coupling to microtubules independently, cooperate to form stronger couplers [87-93]; (2) this process is regulated by Ipl1$^{\text{Aurora B kinase}}$ [89,90,94-97]; (3) Ndc80c transmits force to MIND [98,99], and (4) the kinetochore as a whole behaves as a tension-sensitive catch bond [189]. Load-bearing tip-couplers can form *in vitro* by self-assembly of recombinant Ndc80c [88], MIND [98], and Dam1c [87], demonstrating that these components are sufficient to recapitulate a fundamental function of the outer kinetochore. Relatively little is known about how force is transmitted to the centromeric DNA. It is not even certain which inner kinetochore proteins are involved.

There are only two essential inner kinetochore protein complexes in yeast: Mif2 and OA (Okp1/ Ame1) [112,117,201,202] (**Table 1**). Mif2, the budding yeast homolog of CENP-C, is reported to interact with centromeric nucleosomes [116,118], OA [107], and MIND [99,108,203]. Homologous to human CENP-QU, *S. cerevisiae* OA interacts with Cse4 and MIND, the scaffold that bridges inner and outer kinetochore [95,99,107,108,110]. Because force transmission is a vital function of the kinetochore, I hypothesized that either Mif2 or OA must transmit force through the inner kinetochore.

Using recombinantly purified *S. cerevisiae* proteins, I reconstitute functional kinetochore assemblies capable of tethering centromeric nucleosomes to dynamic microtubule plus-ends. I show that the assemblies are load-bearing, in the sense that they sustain tensile forces in the mitotically relevant piconewton range. In doing so, I demonstrate that there are at least two essential paths of force transmission through the inner kinetochore: the Mif2 and OA protein complexes. Each of these components can independently form load-bearing interactions with both MIND and the centromeric nucleosome.

2.2 METHODS

2.2.1 Plasmids and constructs

All expression vectors are listed in **Table 3**.

Table 3. Plasmids used in this study.

Protein complex	Plasmid name	Proteins expressed*	Vector	References
Mif2	Sc_Mf_7	Mif2-linker-(27-392)MBP-6XHis**	pLIC	This study
	pGH52	Mif2-linker-(27-392)MBP**	pLIC	This study
	Sc_Mf_5B	(41-549)Mif2-linker-(27-392)MBP	pLIC	This study
OA	pGH3	Ame1-6XHis, Okp1	pST39	This study
	pGH4	Ame1-FLAG, Okp1	pST39	This study
	pGH42	(21-324)Ame1-FLAG, Okp1	pST39	This study
	pGH15	(21-324)Ame1-6XHis, Okp1	pST39	This study
MIND	pGH63	6X-His-linker-Nsl1, S240D, S250D-Dsn1, Mtw1, Nnf1	pST39	This study
	pGH62	FLAG-Nsl1, S240D, S250D-Dsn1, Mtw1, Nnf1	pST39	This study
	pGH68	FLAG-Nsl1, (283-576)Dsn1, Mtw1, Nnf1	pST39	This study
	pGH61	FLAG-Nsl1, (230-576)S240D,S250D-Dsn1, Mtw1, Nnf1	pST39	This study
	pGH46	Nsl1, FLAG-Dsn1, Mtw1, Nnf1	pST39	This study
Ndc80c	pJT048	Spc24-Flag, Spc25	pRSFDuet	[98]
	pEM033	Spc24-6XHis, Spc25	pRSFDuet	[86]
	Ndc80/Nuf2	Nuf2, Ndc80	pETDuet	[204]
Dam1c	pJT044	Dad1, Duo1, Spc34-FLAG, Dam1, Hsk3 and Dad4, Dad3, Dad2, Spc19, Ask1‡	pST39	[89]
CI	pGH58	FLAG-Chl4, Iml3	pLIC	This study
Histones	pScKl2	*K.lactis* 6XHis-H2A, *K. lactis* 6XHis-H2B, Cse4, *K. lactis* 6XHis-H4	pLIC	[205]
	pScKl4	H3, 6XHis-H2A, H2B. *K.lactis* 6XHis-H4	pLIC	[205]

*Proteins are listed in order of expression in polycistronic vector. C-terminal tags are given on the right side of the protein name and N-terminal tags on the left side of the protein name.
** Full length Mif2 is expressed by these vectors; the MBP tag includes residues 27-392 of MBP and lacks the signal peptide.
‡Dam1 complex is expressed from two polycistrons in one plasmid.

2.2.2 Protein expression and purification

2.2.2.1 Dam1c, Ndc80c, and MIND

Dam1c, MIND, 2D-MIND, and all MIND truncation mutants were expressed in *Escherichia coli* from polycistronic vectors. Ndc80c was expressed from two bicistronic vectors encoding Ndc80/Nuf2 and Spc24/Spc25 [204]. The protein subcomplexes purified as previously described using either a His_6- or FLAG- affinity tag followed by size exclusion chromatography (SEC) [98,191,206].

Briefly, His_6-tagged protein subcomplexes were expressed from polycistronic pST39 vectors in BL21 cells and induced with 0.4 mM isopropyl β-D-1-thiogalactopyranoside (IPTG) for 16 h at 18 °C. Cells were lysed with a French press and the subcomplex was immobilized on a Ni-charged IMAC resin column (Bio-Rad) in either MIND buffer (50 mM sodium phosphate buffer, pH 7.0, 200 mM NaCl), Ndc80c buffer (50 mM HEPES buffer, pH 7.6, 300 mM NaCl), or Dam1c buffer (50 mM sodium phosphate buffer, pH 6.9, 500 mM NaCl) supplemented with protease inhibitors (Roche), 5 mM imidazole, and 1 mM PMSF. The resin was then washed, and subcomplex eluted with 300 mM imidazole before being further purified using a Superdex 200 size exclusion column (GE Healthcare) in either MIND buffer, Ndc80c buffer with 200 mM NaCl, or Dam1c buffer.

2.2.2.2 OA

Wild-type (WT) and truncated His_6-tagged OA was expressed in a polycistronic pST39 vector in BL21 cells and induced with 0.4 mM IPTG for 16 h at 18 °C. Cells were lysed with a French press and OA was immobilized on a Ni-charged IMAC resin column (Bio-Rad) in 50 mM sodium phosphate buffer, pH 7.0 supplemented with 200 mM NaCl, protease inhibitors (Roche), 5 mM imidazole, and 1 mM PMSF, washed, and eluted in the same buffer with 300 mM imidazole. OA was further purified using a Superdex 200 size exclusion column (GE Healthcare) in 50 mM sodium phosphate buffer, pH 7.0 supplemented with 200 mM NaCl.

WT and truncated FLAG-tagged OA was expressed similarly to His_6-tagged OA except that it was immobilized on an anti-FLAG M2 affinity gel (A2220; Sigma). The affinity gel was washed, and protein was eluted with 0.1 $mg \cdot mL^{-1}$ 3X FLAG Peptide (F4799; Sigma). OA was further purified using a Superdex 200 size exclusion column (GE Healthcare) in SEC-OA buffer.

After SEC, OA was concentrated with Amicon Ultra centrifugal filters (Millipore), stored in SEC-OA buffer with 5% glycerol, and immediately stored at -80°C.

2.2.2.3 Mif2

Full length Mif2-C-terminal(Ct)MBP tag and Mif2-(Ct)MBP-His_6 constructs were expressed in Rosetta 2 DE3 pLysS competent cells (Novagen) and expression was induced with 0.25 mM IPTG at 18°C for 16 h. Cells were lysed with either sonication or a French press. Mif2-(Ct)MBP was immobilized on amylose resin (NEB) in Mf1-buffer (30 mM HEPES buffer, pH 7.5, 2 M NaCl, 10% glycerol, 1 mM TCEP, protease inhibitors (Roche) and 1 mM PMSF). The column was washed with Mf1-buffer and the protein eluted with Mf1-buffer containing 10 mM maltose. Protein samples were immediately loaded on HiTrap Q HP (GE Healthcare) anion exchange column in buffer QA (30 mM HEPES buffer, pH 7.5, 50 mM NaCl, 1 mM TCEP, 10% glycerol) and eluted with a 0-100% gradient of buffer QB (30 mM HEPES buffer, pH 7.5, 1 M NaCl, 1 mM TCEP, 10% glycerol). This was followed by SEC on a preparative Superdex200 HiLoad 16/60 column (GE Healthcare) in SEC-Mif2 buffer (30 mM HEPES buffer, pH 7.5, 200 mM NaCl, 1mM TCEP). Purification of all Mif2 constructs was performed at 4°C to prevent protein degradation. Mif2 protein was immediately concentrated, frozen, and stored at -80°C.

2.2.2.4 Chl4/Iml3

CI was expressed from a bicistronic vector (derived from pSMH104) in Rosetta DE3 pLysS competent cells (Novagen) and expression induced with 0.25 mM IPTG as previously described [207]. Cells were lysed with a French press. CI was immobilized on anti-FLAG M2 affinity resin (Sigma) in CI-buffer of 50 mM HEPES buffer, pH 7.5, 100 mM NaCl, 1 mM EDTA, 10% glycerol, protease inhibitors (Roche) and 1 mM PMSF. The affinity gel was washed, and protein was eluted with SEC-CI buffer (50 mM Tris buffer, pH 8.5, 200 mM NaCl, 1mM TCEP) supplemented with 0.1 $mg \cdot mL^{-1}$ 3X FLAG Peptide (F4799; Sigma). CI was further purified using a Superdex 200 size exclusion column (GE Healthcare) in SEC-CI buffer (50mM Tris-Cl, pH = 8.5, 200mM NaCl and 1mM TCEP). After SEC, all proteins were concentrated with Amicon Ultra centrifugal filters (Millipore), stored in SEC-CI buffer from the final Superdex 200 run with 5% glycerol, and immediately stored at -80°C.

2.2.2.5 Nucleosome core particles (NCPs)

Each histone complex was co-expressed from a single expression polycistronic vector encoding *S.cerevisiae (Sc)* and *Kluyveromyces lactis (Kl)* genes: pScKl2 containing His_6-*Kl*-H2A / His_6-*Kl*-H2B / *Sc*-Cse4 / His_6-*Kl*-H4 and pScKl4 containing *Sc*-H3 / His_6-*Sc*-H2A / *Sc*-H2B / His_6-*Kl*-H4 [205]. Histones were co-expressed from pScKl2 or pScKl4 in Rosetta 2 DE3 pLysS competent cells (Novagen) and upon reaching OD_{600} of 0.6-1.0, expression was induced with 0.25 – 0.5 mM IPTG and cells grown for 16 h at 18°C. Cells were resuspended in High Salt Buffer (HSB) of 2 M NaCl, 50 mM HEPES buffer, pH 7.5, 10% glycerol, 1 mM TCEP and protease inhibitors (aprotonin, pepstatin, leupeptin, and PSMF), frozen and stored at –80°C. Cells were lysed by sonication and lysate clarified by centrifugation at 40,000xg at 4°C for 1 h. Histones were immobilized on TALON metal affinity resin (Clontech) and incubated at 4°C for 1 h with agitation, then transferred to a gravity column.

The flowthrough was discarded, beads washed with HSB, and histones eluted with 400 mM imidazole and 50 mM EDTA. The eluate was concentrated, and histone octamers were further purified on a Superdex 200 size exclusion column (GE Healthcare) in SEC-H1 buffer containing 2M NaCl, 50 mM HEPES buffer, pH 7.5, 1 mM TCEP.

Histone octamers were wrapped in the 147-basepair double-stranded Widom DNA (henceforth “601 DNA") [208] as described [205] 601 DNA was produced by PCR and final purification performed using HiTrapQ column. 601 DNA and histone octamers were combined in a 1.1:1 molar ratio in a hydrated 7K MWCO Slide-A-Lyzer™ MINI Dialysis Device (69560; ThermoFisher), which was placed in 0.5 L of high-salt dialysis buffer (2 M NaCl, 30 mM HEPES buffer, pH 7.5, 1 mM TCEP, and 5 mM EDTA). The nucleosome wrapping was achieved through dialysis against low salt dialysis buffer (200 mM NaCl, 30 mM HEPES buffer, pH 7.5, 1 mM TCEP, and 5 mM EDTA) over the course of 60 h at 4°C. Wrapped nucleosomes were separated from excess DNA using a Superdex 200 or Superdex 6 size exclusion columns (GE Healthcare) with SEC-H2 buffer 150 mM NaCl, 30 mM HEPES buffer, pH 7.5, 1 mM TCEP. NCPs were stored on ice, and all experiments using NCPs were performed within one week of wrapping.

2.2.3 Optical trap assays

Streptavidin-coated 0.56-μm polystyrene beads (Spherotech) were coated with biotinylated anti-His5 antibodies (Qiagen), and 7 pM beads were incubated with 10 nM His_6-tagged protein complex as described [206] [161] [89], such that each bead was decorated with ~3,000 protein complexes. Flow cells were prepared using double-sided tape and plasma-cleaned coverslips and incubated with 25 μL of 1 $mg \cdot mL^{-1}$ biotinylated BSA (Vector Laboratories) for 15 min at room temperature, then washed with BRB80 (80 mM PIPES, pH 6.9, 1 mM $MgCl_2$, 1 mM EGTA). Flow cells were then incubated with 30 μL of 1 $mg \cdot mL^{-1}$ avidin DN (Vector Laboratories) for 5 min at room temperature, followed by another BRB80 wash. GMPCPP biotinylated tubulin seeds in BRB80 were bound for 5 min and washed twice with 42°C growth buffer (BRB80 plus 1 mM GTP and 105 μM κ-casein). Protein-decorated beads were introduced into the flow chamber in growth buffer with 1.4 $mg \cdot mL^{-1}$ tubulin, 313 $\mu g \cdot mL^{-1}$ glucose oxidase, 37.5 $\mu g \cdot mL^{-1}$ catalase, 30 mM glucose, 1 mM DTT, and 10 nM each of the free, non-His-tagged protein complexes.

For the negative controls (e.g., OA-decorated beads with Ndc80c but not MIND in solution), all beads and soluble proteins were maintained at the concentrations used in the experimental reactions, except for the subcomplex being omitted.

For each condition, a bead was manipulated to make contact with a microtubule (**Figure 2-1**). If the bead-microtubule contact did not persist after the laser was switched off, that bead was considered to be a nonbinder. Optical trap assays were performed at room temperature using custom instrumentation to capture and manipulate beads as described [206]. Rupture force assays were performed as described [91,97,189]. Once beads were bound to microtubule tips, a test force of 1 pN was applied, and only beads that tracked with ~100 nm of tip growth were subjected to ramping force of 0.25 $pN \cdot s^{-1}$ until detachment. Records of force vs. time were collected, and maximum rupture force was determined using custom Igor Pro software (Wavemetrics). Protein chains that withstood the 1-pN preload force were considered load-bearing, and rupture forces were used to compare relative mechanical strength.

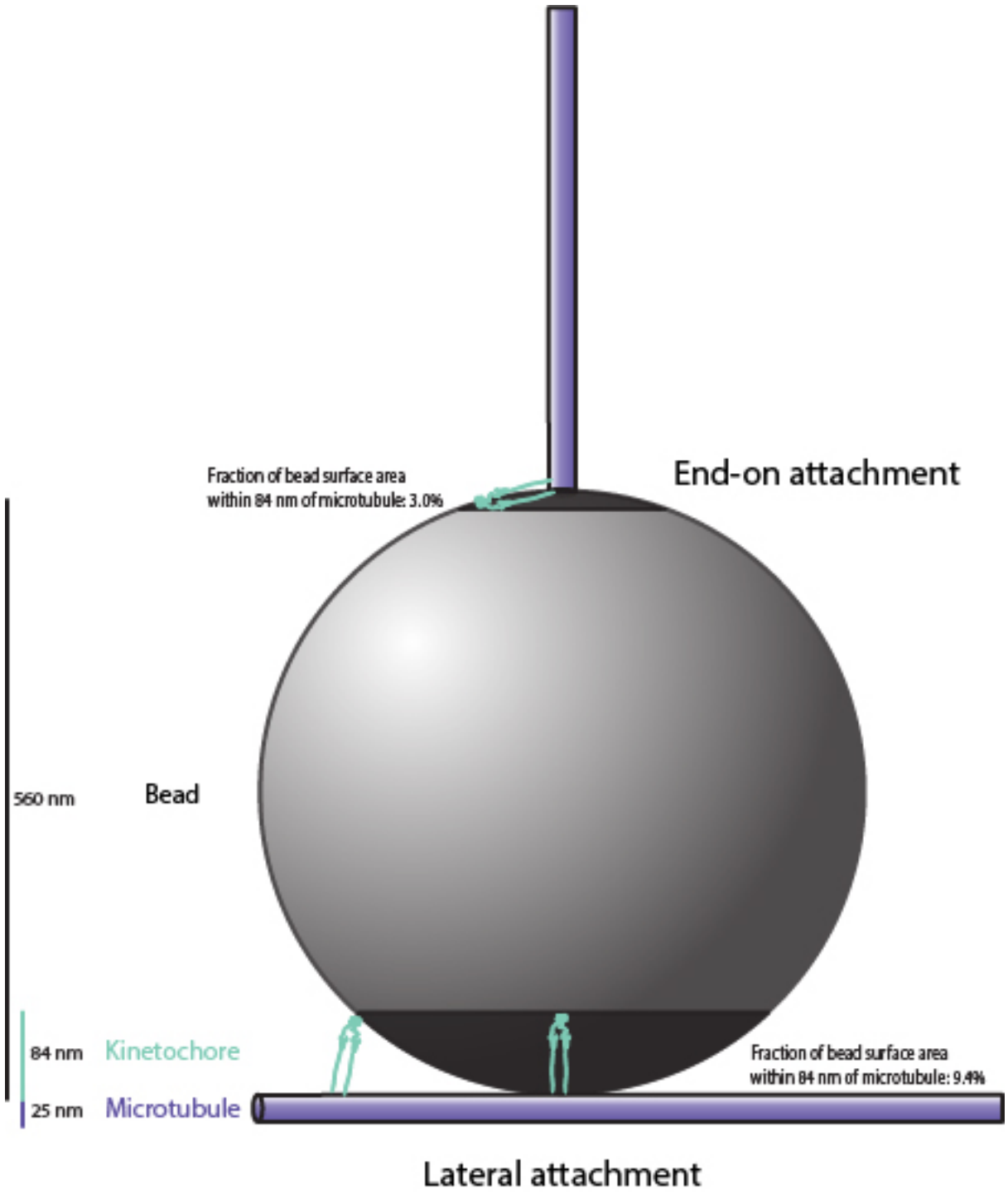

Figure 2-1. Schematic diagram, drawn approximately to scale, showing the two possible bead-microtubule configurations. Our rupture force assay quantifies the strength of end-on attachments. In this configuration, reconstituted kinetochores on only ~3.0% of the bead surface are capable of simultaneously binding to the microtubule. Assuming that the ~2900 protein complexes on each bead are evenly distributed, ~86 would be capable of binding the microtubule surface. Lateral attachments likely predominate in self-assembly and microtubule-binding assay. In this configuration, the bead rests against the side of a filament whose tip extends well past the

point of contact, maximizing the amount of bead surface in close proximity to the microtubule. Thus, it provides an upper limit for the fraction of bead surface within 84 nm of the microtubule. Reconstituted kinetochores on ~9.4% of the bead surface, ~270 protein complexes, are capable of simultaneously binding to the microtubule.*Data analysis and figure preparation*

Data were analyzed in R [209-211] and Igor Pro (Wavemetrics). Because only a small number of planned comparisons were made, each to test a specific hypothesis, p-values were not adjusted for multiple comparisons. Figures were produced using R and Adobe Illustrator.

2.3 RESULTS

2.3.1 Assay to test quantitatively for spontaneous self-assembly of purified kinetochore subcomplexes

The proteins of the *S. cerevisiae* kinetochore are organized into subcomplexes (**Figure 2-2A**). I have recombinantly expressed and purified seven of these complexes in *E. coli* and isolated bovine brain tubulin to allow reconstitution and mechanical testing of functional kinetochore assemblies *in vitro* (**Figure 2-2B**). Previously, my colleagues in the Davis Lab showed that the microtubule-binding Ndc80c and Dam1c complexes, when introduced free in solution, will associate with bead-bound MIND to form load-bearing attachments to dynamic microtubule tips [98]. I have now extended this approach to test longer protein chains, including both inner and outer kinetochore components (**Figure 2-2C**). In order to test a protein chain containing multiple components, one subcomplex carrying a His6-tag was bound directly to polystyrene microbeads via anti-His antibodies. The remaining subcomplexes, which did not have His_6-tags, were added free in solution and bound to the beads only indirectly, by assembling together with the directly tethered, His_6-tagged subcomplex. Using a laser trap to manipulate individual beads, the kinetochore assemblies were tested for their ability to couple to assembling microtubule tips. If they attached, then their coupling strength was subsequently measured by increasing the force until

they detached from the tips [87,88,189,206] (**Figure 2-2D**). In negative controls, microtubule coupling was abrogated by omitting one of the non-His_6-tagged subcomplexes.

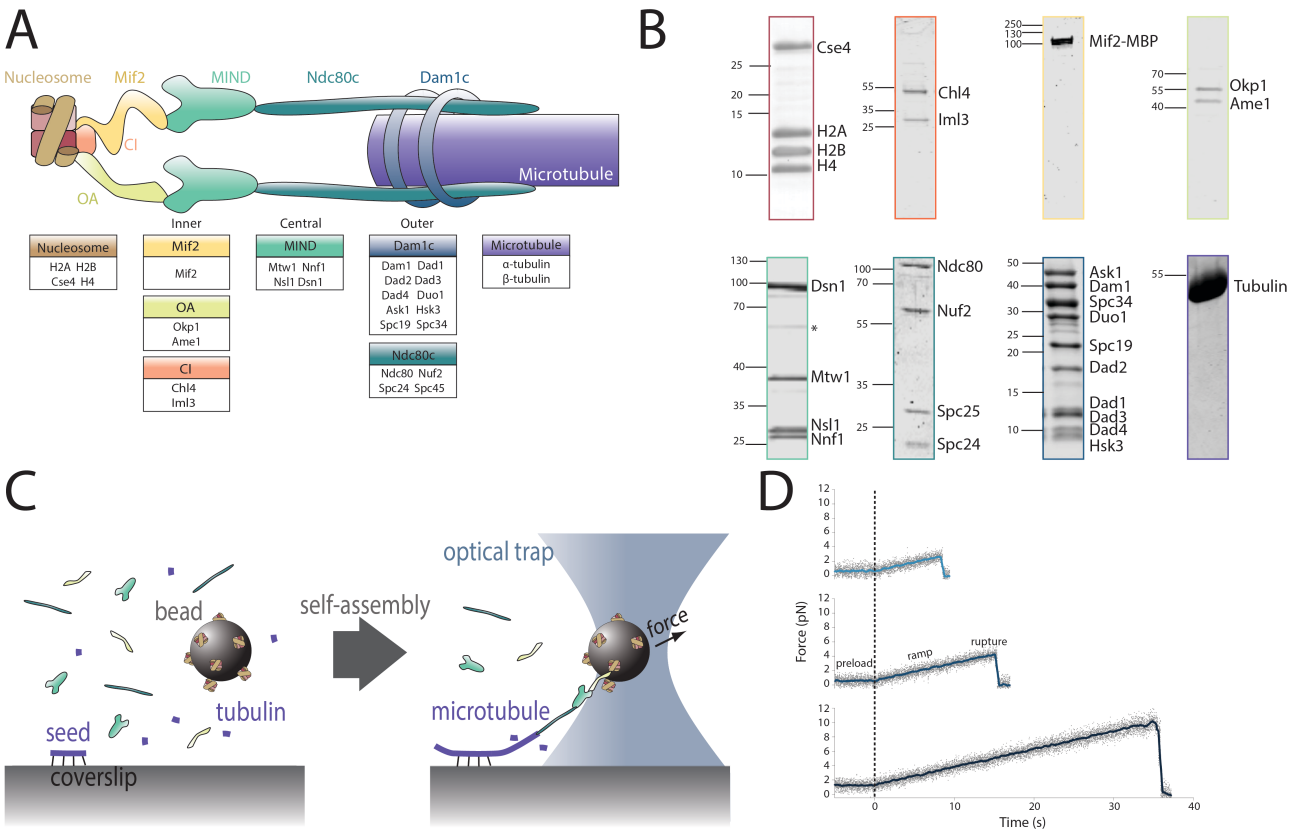

Figure 2-2. Reconstitution of a kinetochore from individually purified parts and an optical trap-based assay to test for self-assembly of functional chains of kinetochore subcomplexes. (A) Schematic of the protein complexes of the budding yeast kinetochore. (B) Coomassie-stained SDS-PAGE gel of heterologously expressed budding yeast kinetochore proteins. The asterisk indicates a contaminating *E. coli* protein or degradation product. (C) Schematic of the optical trap assay used to test for assembly and microtubule attachment prior to quantification of load-bearing ability. (D) Representative force vs. time traces for ruptures in the force-ramp assay.

2.3.2 OA forms microtubule attachments through MIND and Ndc80c

Both of the two essential inner kinetochore protein complexes, Mif2 and OA, bind directly to MIND [99,107]. Thus I began by asking whether OA could form a microtubule attachments through MIND and Ndc80c. With OA bound to the polystyrene beads, and MIND and Ndc80c added in solution (at 10 nM), the vast majority of beads coupled to assembling microtubule tips,

indicating that functional, OA-based co-complexes spontaneously assembled *in vitro* (**Figure 2-3A**).

No microtubule attachments were observed if MIND was omitted from the assay, demonstrating that OA must interact specifically through MIND – and not with Ndc80c or the microtubule directly – in order for the microtubule-coupling assemblies to form. Likewise, very few beads attached (6%) when they were decorated with a truncated mutant OA complex (ΔOA), lacking the N-terminal 20 residues of Ame1 that bind the MIND complex [99,107,203] (**Figure 2-3A**). Together with the prior observation that MIND itself has no microtubule-binding activity [98], these results indicate that a three-component chain, OA/MIND/Ndc80c, spontaneously assembles to couple OA indirectly to the microtubule tip. This arrangement is consistent with localization dependencies seen *in vivo* [77], co-immunoprecipitation (co-IP) dependencies [77,104], and with previous *in vitro* reconstitutions of metazoan kinetochore proteins [95,194].

Phosphorylation of two sites on Dsn1 has been shown to alleviate an intra-complex autoinhibition, thereby allowing MIND to interact more stably with both OA and Mif2 [99,108]. However, I found that both the wild-type MIND complex and a phosphomimetic mutant, 2D-MIND, carrying aspartic acid substitutions at the two target phosphorylation sites on Dsn1 (S240D, S250D), supported the attachment of a similarly high fraction of OA-coated beads to assembling microtubule tips (**Figure 2-3A**). This observation suggests that the intra-complex autoinhibition within MIND does not abrogate its interaction with OA.

2.3.3 OA forms a load-bearing attachment to MIND

Because tip-coupled kinetochores must support piconewton-scale loads *in vivo*, I asked whether the reconstituted OA/MIND/Ndc80c chains could support such loads *in vitro*. In order to quantify their load-bearing ability, I used a force-ramp assay [206]. After attachment of a bead to a growing microtubule tip and application of a weak preload force (~1 pN), the force was gradually increased (at 0.25 pN s^{-1}) until the attachment ruptured. The median rupture strength of tip-attachments formed by OA/MIND/Ndc80c chains was 3.0 pN (**Figure 2-3B and C**), indicating that both the OA/MIND and MIND/Ndc80c interfaces can bear load. When the phosphomimetic 2D-MIND was used instead of wild-type MIND, the median rupture strength of the OA/2D-MIND/Ndc80c chains increased slightly, to 3.9 pN. This observation suggests that the

autoinhibition within the MIND complex slightly weakens the load-bearing capacity of the OA/MIND interface.

While rupture strengths by themselves do not provide information about which protein-protein interface breaks for each rupture, some inferences can be made from comparative analysis. For example, previously published work demonstrates that MIND/Ndc80c-mediated microtubule attachments do not differ in strength from Ndc80c-mediated attachments [98], implying that the MIND/Ndc80c interface is mechanically stronger than the Ndc80c/microtubule interface. This conclusion was additionally supported by the prior observation that adding Dam1c, which specifically strengthens the Ndc80c/microtubule interface, significantly increases the strength of MIND/Ndc80c-mediated attachments [98]. In order to determine if the OA/MIND interface is likewise mechanically strong relative to the Ndc80c/microtubule interface, I specifically strengthened the latter by adding Dam1c in solution to our rupture force assay. OA/MIND/Ndc80c-mediated attachments nearly doubled in strength, to a median rupture force of 7.6 pN, with the addition of Dam1c (**Figure 2-3B and C**). This suggests that the OA/MIND interface, like the MIND/Ndc80c interface, is mechanically strong relative to the Ndc80c/microtubule interface.

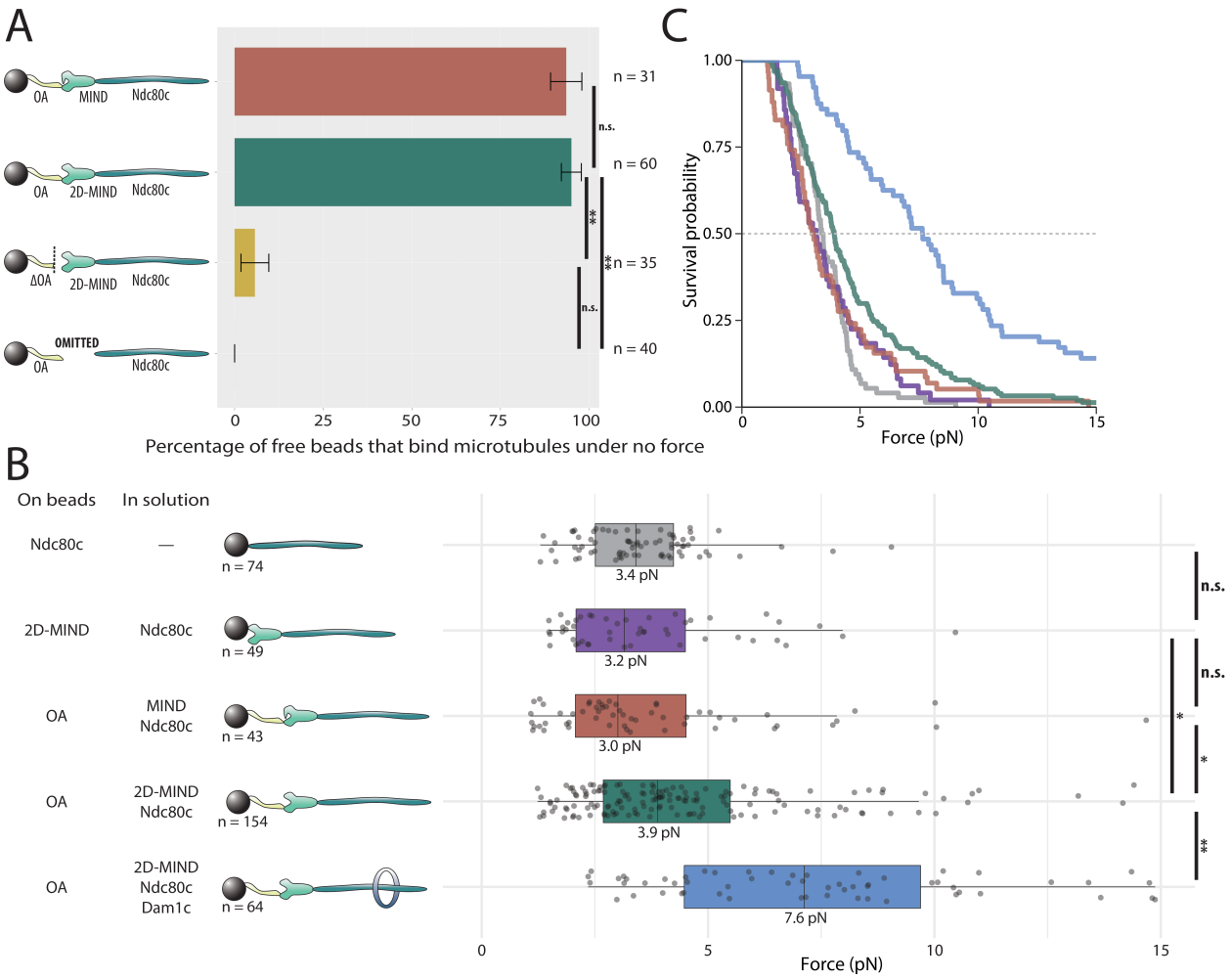

Figure 2-3. OA-based chains assemble spontaneously and form load-bearing attachments to dynamic microtubules. (A) Percentage of free beads that bound microtubules under no external force. Error bars indicate the standard error of the sample proportion. Barnard's test was used to compare contingency tables. n.s. indicates $p > 0.05$. * indicates $p < 0.05$. ** indicates $p < 0.01$. (B) Boxplot of rupture forces observed with reconstituted kinetochores of increasing length. Each shaded circle is an individual rupture event. Boxes extend from the lower quartile to the upper quartile. Whiskers extend to 1.5 times the interquartile range beyond each quartile. A Kolmogorov-Smirnov test was used to compare probability distributions and calculate p-values. n.s. indicates $p > 0.05$. * indicates $p < 0.05$. ** indicates $p < 0.01$. (C) Survival curves for **Ndc80c linkages (grey)**, **MIND/Ndc80c linkages (purple)**, **OA/MIND/Ndc80c linkages (pink)**, **OA/2D-MIND/Ndc80c linkages (turquoise)**, and **OA/2D-MIND/Ndc80c/Dam1c linkages (blue)**. The dashed horizontal line indicates 50% survival (median rupture force).

2.3.4 Mif2 forms microtubule attachments through MIND and Ndc80c

I then asked if Mif2 could form microtubule attachments through MIND and Ndc80c. Mif2 was bound to polystyrene beads, while wild-type MIND and Ndc80c were added in solution. A substantial fraction of the beads, 45%, coupled to microtubule tips, demonstrating that functional, three-component Mif2/MIND/Ndc80c chains spontaneously assembled *in vitro* (**Figure 2-4A**). Hypothesizing that intra-complex autoinhibition within MIND might be responsible for the 55% of beads that failed to bind microtubules, I repeated the same experiment, but using the phosphomimetic mutant, 2D-MIND, instead of wild-type MIND. With this substitution, the fraction of Mif2-coated beads capable of coupling to microtubules increased to 81% (**Figure 2-4A**), suggesting that intra-complex autoinhibition within MIND tightly regulates its interaction with Mif2. To confirm that 2D-MIND was essential for connecting Mif2 to Ndc80c, I omitted 2D-MIND from the assay. Beads coated in Mif2 did not couple to microtubules in the absence of MIND (**Figure 2-4A**), indicating that Mif2, like OA (**Figure 2-3A**), must bind directly to 2D-MIND, and not to Ndc80c or to microtubules. Unlike OA, however, Mif2 requires alleviation of autoinhibition within the MIND complex in order to bind tightly. For this reason, 2D-MIND was used in all subsequent experiments.

The conserved N-terminus of Mif2 is sufficient for binding to the Dsn1/Nsl1 head of the MIND complex [99,107,203]. In order to probe the specific Mif2 domains involved in assembling functional microtubule-coupling chains, I purified a truncated version lacking the first 40 N-terminal residues, ΔMif2. Only 16% of beads coated with ΔMif2 interacted with microtubules (**Figure 2-4A**), suggesting that the N-terminal domain of Mif2, like the N-terminus of Ame1, is an important point of attachment between the inner kinetochore and MIND. But because a significant fraction of beads was still able to bind microtubules in the absence of the first 40 residues of Mif2, it seems likely that other amino acids also contribute to the Mif2/MIND interface, as seen in the case of CENP-C/Mis12 complex [94].

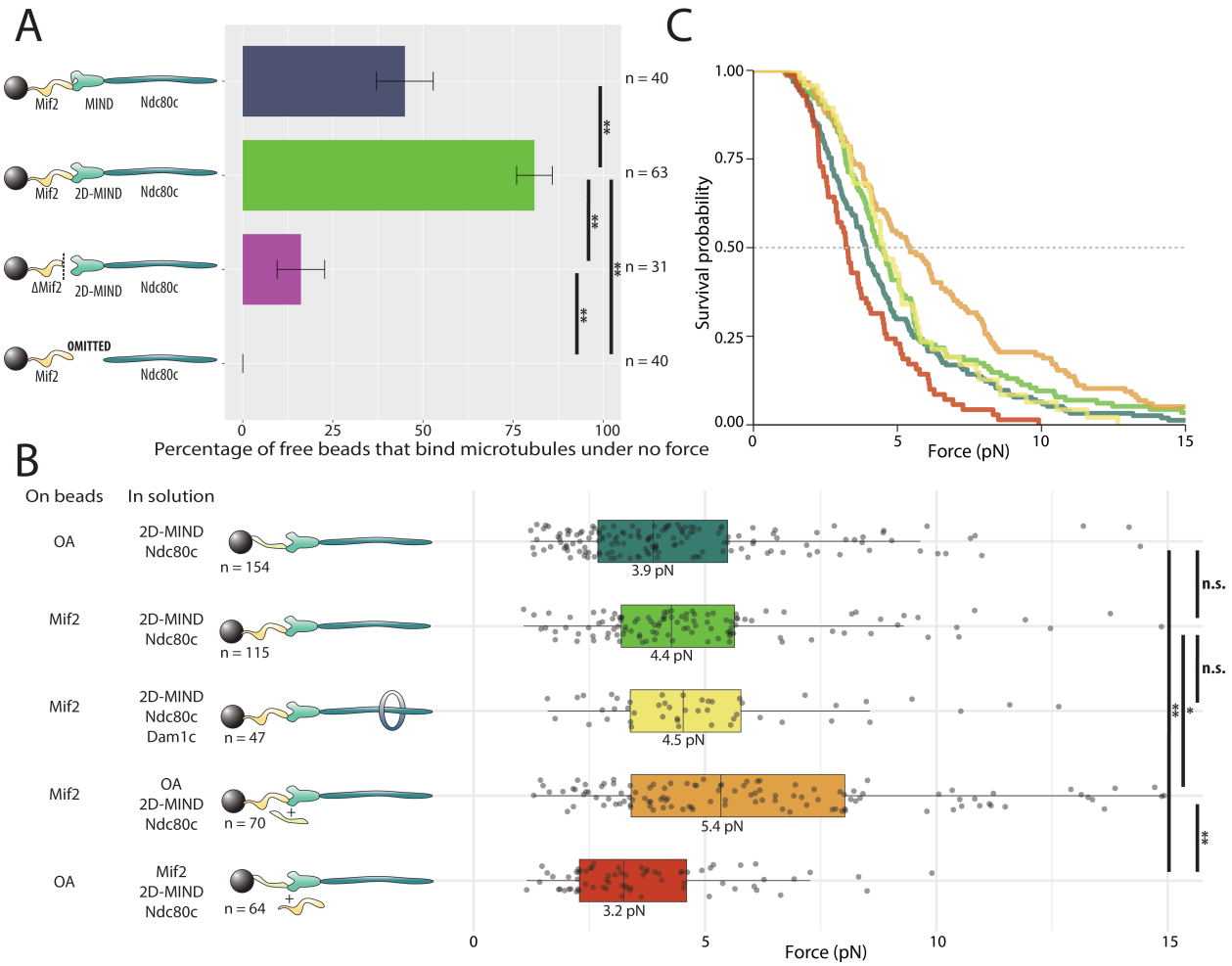

Figure 2-4. Mif2-based chains also assemble spontaneously and form load-bearing attachments to dynamic microtubule tips. (A) Percentage of free beads that bound microtubules under no force. Error bars indicate the standard error of the sample proportion. Barnard's test was used to compare contingency tables. n.s. indicates $p > 0.05$. * indicates $p < 0.05$. ** indicates $p < 0.01$. "2D" indicates that two phosphomimetic mutations (S240D, S250D) have been made to the MIND component Dsn1. (B) Boxplot of rupture forces observed with reconstituted kinetochores. Each shaded circle is an individual rupture event. Boxes extend from the lower quartile to the upper quartile. Whiskers extend to 1.5 times the interquartile range beyond each quartile. A Kolmogorov-Smirnov test was used to compare probability distributions and calculate p-values. n.s. indicates $p > 0.05$. * indicates $p < 0.05$. ** indicates $p < 0.01$. (C) Survival curves for **OA/2D-MIND/Ndc80c linkages (turquoise**, repeated from Figure 2-3 for comparison), **Mif2/2D-MIND/Ndc80c linkages (green)**, **Mif2/MIND/Ndc80c/Dam1c linkages (yellow)**, **Mif2/OA/MIND/Ndc80c linkages (orange)**, and **OA/Mif2/MIND/Ndc80c linkages (red)**. The dashed horizontal line indicates 50% survival (median rupture force).

2.3.5 Mif2 forms a load-bearing attachment to MIND

To quantify the rupture strength of Mif2-based assemblies, I applied the force-ramp assay. Mif2/2D-MIND/Ndc80c-mediated attachments ruptured at 4.4 pN, indicating that they support piconewton-scale loads. Notably, their strength was not significantly different from the 3.9 pN median rupture strength I measured for OA-based assemblies (**Figure 2-4B and C**). As explained above, the addition of Dam1c significantly strengthened OA-based linkers, indicating that the OA/MIND interface is mechanically strong relative to the Ndc80c/microtubule interface. To ask if the same is true of the Mif2/MIND interface, I tested whether Mif2/2D-MIND/Ndc80c chains could be strengthened by the addition of Dam1c. In contrast to our results with OA, adding Dam1c had no significant effect ($p = 0.67$) on the strength of the Mif2-based chains (**Figure 2-4B and C**). This observation suggests that the OA/MIND interface is mechanically strong relative to the Ndc80c/microtubule attachment, but that the Mif2/MIND interface is not.

Having demonstrated that both Mif2 and OA can independently transmit force to MIND, I then asked if these two subcomplexes are stronger in combination. I added free OA to the Mif2/2D-MIND/Ndc80c chain, thereby increasing its median rupture force from 4.4 pN to 5.4 pN (**Figure 2-4B and C**). This increase suggests that OA is able to strengthen the Mif2/MIND interface, which I believe is relatively weak (based on our experiments with Dam1c). In OA-based linkers, on the other hand, the OA/MIND interface was not the weakest link, leading to the prediction that strengthening that interface should not increase median rupture force. Indeed, the addition of Mif2 in solution did not strengthen OA/2D-MIND/Ndc80c-mediated attachments (**Figure 2-4B and C**), consistent with our earlier inference that the Ndc80c/microtubule interface is usually the site of rupture in our OA-based assemblies.

2.3.6 Both OA and Mif2 assemble with centromeric nucleosomes

Previous work shows that Mif2 and OA can bind centromeric nucleosomes [110,116,118,212], which carry a specialized variant of histone H3 ($Cse4^{CENP\text{-}A}$) [213,214]. To ask if either Mif2 or OA can assemble in our assay onto these specialized nucleosomes, histone complexes containing H2A, H2B, H4, and Cse4, the centromere-specific H3 variant from *S. cerevisiae*, were wrapped in 601 DNA and the resulting nucleosome core particles (Cse4-NCPs) were bound to polystyrene microbeads. Mif2 or OA was then added in solution, along with 2D-

MIND and Ndc80c. With OA in solution, 78% of beads bound microtubules; with Mif2 in solution, 24% bound (**Figure 2-5A**). Possible reasons for the relatively low percentage of active Cse4-NCP-decorated beads in the experiments with added Mif2/2D-MIND/Ndc80c are discussed below. Nevertheless, these observations confirm that OA and Mif2 can individually link the outer kinetochore subcomplexes, 2D-MIND/Ndc80c, to centromeric nucleosomes, spontaneously forming the four-component microtubule-binding chains, Cse4-NCPs/OA/2D-MIND/Ndc80c and Cse4-NCPs/Mif2/2D-MIND/Ndc80c, respectively. As expected [104], the Cse4-NCP-decorated beads completely failed to bind microtubules if both OA and Mif2 were omitted (**Figure 2-5A**), confirming that the NCPs themselves do not interact directly with MIND, Ndc80c, or microtubules. To ask whether Mif2 and OA bind specifically to *centromeric* nucleosomes, my collaborator also wrapped canonical nucleosomes containing histone H3 (instead of Cse4) with 601 DNA, and I attached these H3-NCPs to beads. The H3-NCP-decorated beads did not bind microtubules with either Mif2 or OA in solution (**Figure 2-5A**), indicating that both Mif2 and OA bind selectively to centromeric, Cse4-containing nucleosomes. Their selectivity is striking given that *S. cerevisiae* H3 and Cse4 are 46 % identical. Altogether these results show that Mif2 and OA represent the molecular bases for two distinct paths connecting the outer kinetochore to the centromere.

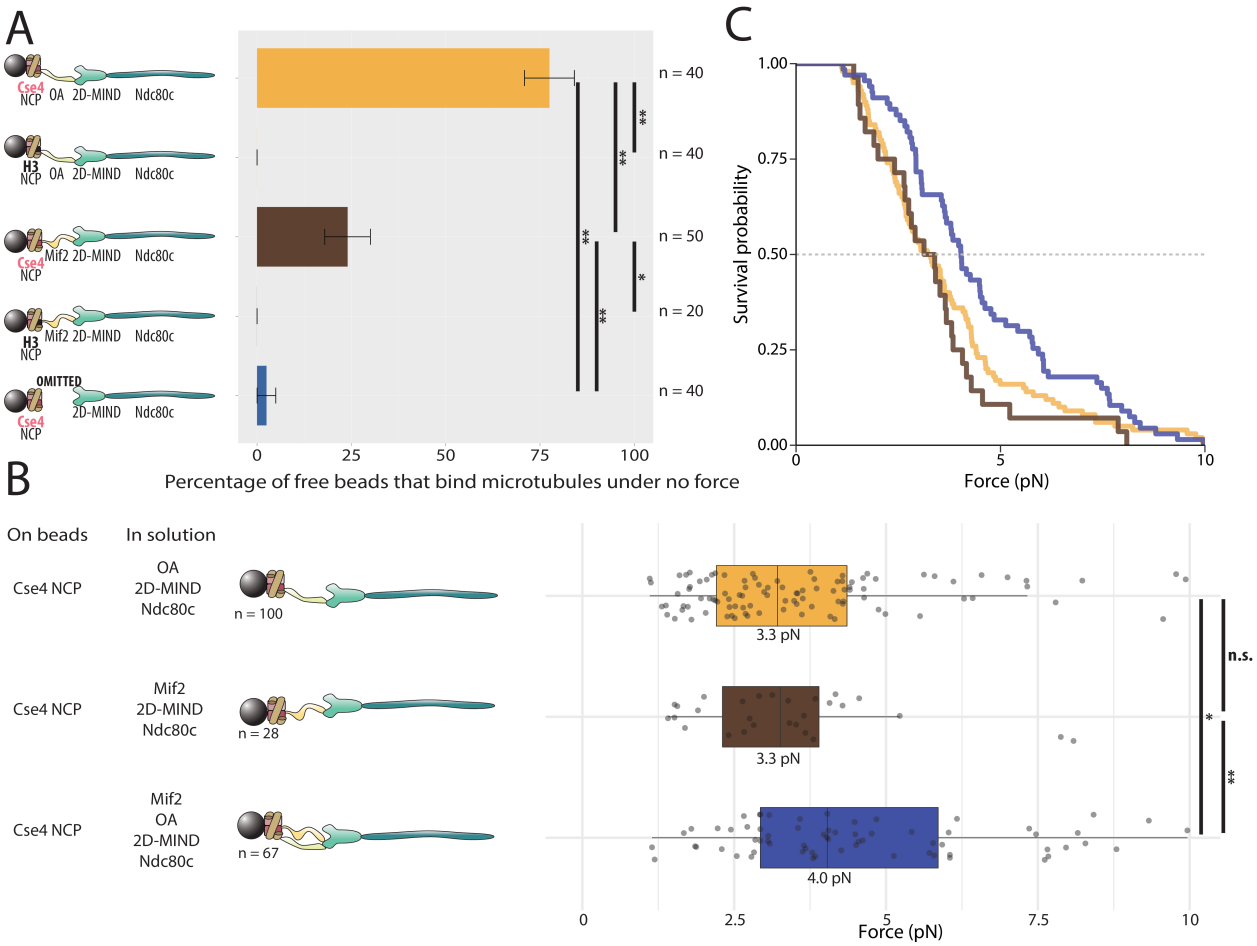

Figure 2-5. Assemblies based on centromeric nucleosomes form load-bearing microtubule attachments through OA or Mif2 or both. (A) Percentage of free beads that bound microtubules under no force. Error bars indicate the standard error of the sample proportion. Barnard's test was used to compare contingency tables. n.s. indicates $p > 0.05$. * indicates $p < 0.05$. ** indicates $p < 0.01$. (B) Boxplot of rupture forces observed with reconstituted kinetochores. Each shaded circle is an individual rupture event. Boxes extend from the lower quartile to the upper quartile. Whiskers extend to 1.5 times the interquartile range beyond each quartile. A Kolmogorov-Smirnov test was used to compare probability distributions and calculate p-values. n.s. indicates $p > 0.05$. * indicates $p < 0.05$. ** indicates $p < 0.01$. (C) Survival curves for **Cse4 NCP/OA/2D-MIND/Ndc80c linkages (yellow)**, **Cse4 NCP/ Mif2/2D-MIND/Ndc80c linkages (brown)**, and **Cse4 NCP/OA/Mif2/2D-MIND/Ndc80c linkages (purple)**.

2.3.7 Both OA and Mif2 form load-bearing attachments to centromeric nucleosomes

Having established that both OA and Mif2 can individually and selectively link bead-bound Cse4-NCPs to outer kinetochore subcomplexes, I used our force-ramp assay to test whether these interactions are load-bearing. With Cse4-NCPs on the beads, attachments mediated by Cse4-NCP/Mif2/2D-MIND/Ndc80c chains ruptured at 3.3 pN (**Figure 2-5B and C**). Likewise,

attachments mediated by Cse4-NCP/OA/2D-MIND/Ndc80c chains also ruptured at 3.3 pN. The two survival curves are not significantly different from one another ($p = 0.55$) (**Figure 2-5B**). However, both are significantly weaker than the chains assembled with Mif2 or OA bound directly to the beads, without NCPs ($p = 0.00015$ for the comparison with Mif2/2D-MIND/Ndc80c; $p = 0.00405$ for OA/2D-MIND/Ndc80c).

Given our previous finding that OA strengthens Mif2-based chains (**Figure 2-4B and C**), I was curious whether the simultaneous presence of both inner kinetochore complexes, OA and Mif2, would strengthen Cse4-NCP-based chains. It did. Cse4-NCP-based chains with both Mif2 and OA added in solution were significantly stronger than chains containing only Mif2 ($p = 0.015$) or containing only OA ($p = 0.037$) (**Figure 2-5B and C**). This strengthening suggests that the Mif2/Cse4-NCP and OA/Cse4-NCP interfaces created in our assay are individually relatively weak, but can mutually reinforce one another. To further assess the relative strength of the OA/Cse4-NCP interface, I added free Dam1c to the Cse4-NCP/OA/2D-MIND/Ndc80c chains (**Figure 2-6A and B**). The addition of Dam1c, which specifically strengthens the Ndc80/microtubule interface, had no significant effect on the median rupture force of the Cse4-NCP/OA/2D-MIND/Ndc80c chains ($p > 0.5$), indicating that the Cse4-NCP/OA interface is probably the weakest link in these chains. I attempted to strengthen that interface by adding CI in solution, but it also had no effect on the median rupture force ($p > 0.5$) (**Figure 2-6A and B**). Altogether, these data indicate that both essential components of the inner kinetochore, OA and Mif2, are capable of independently transmitting piconewton-scale forces from the outer kinetochore to centromeric nucleosomes.

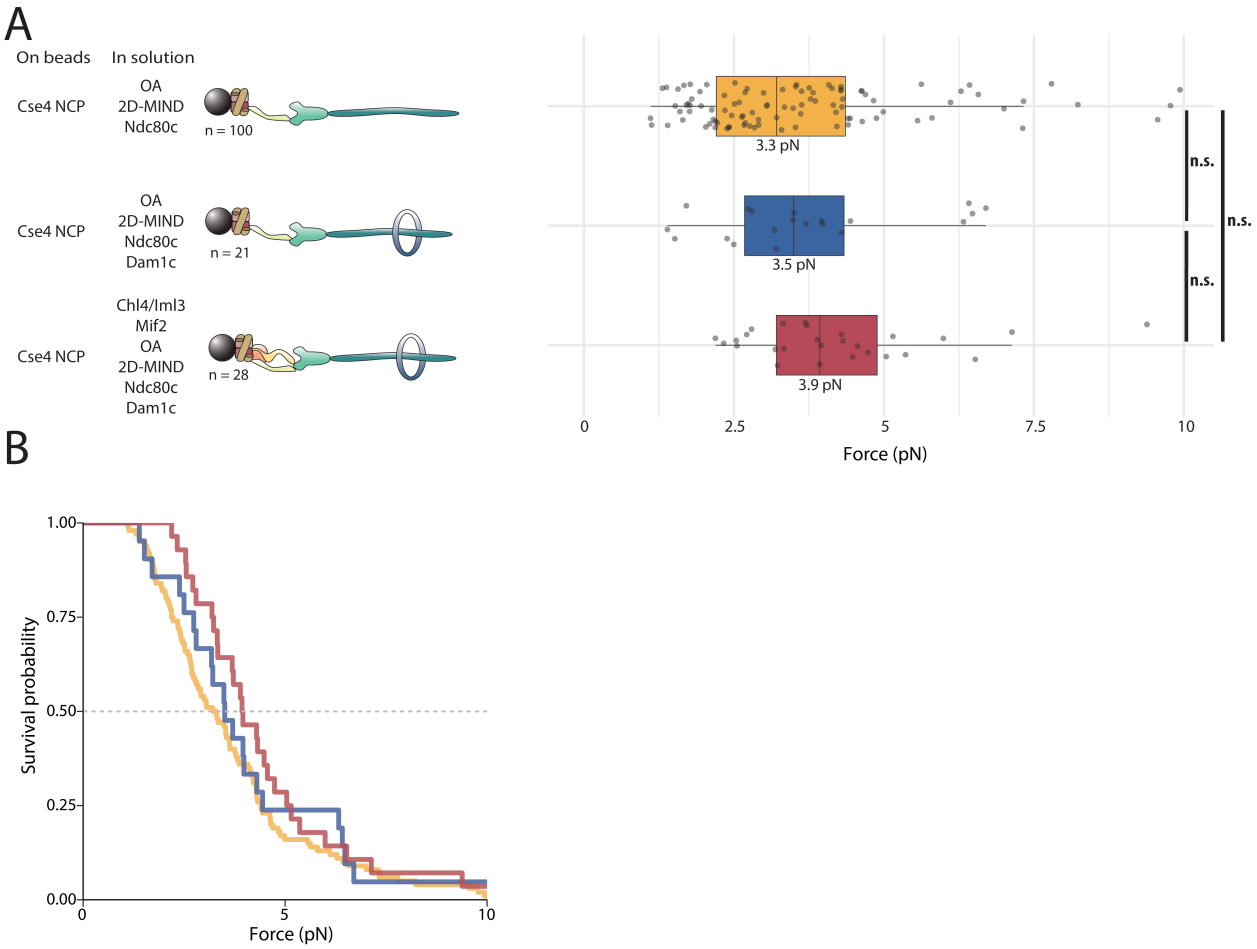

Figure 2-6. Neither Dam1c nor CI increases the rupture force of NCP-containing linkers. (A) Boxplot of rupture forces observed with reconstituted kinetochores. Each shaded circle is an individual rupture event. Boxes extend from the lower quartile to the upper quartile. Whiskers extend to 1.5 times the interquartile range beyond each quartile. A Kolmogorov-Smirnov test was used to compare probability distributions and calculate p-values. * indicates $p < 0.05$. (B) Survival curves for **Cse4-NCP/ OA/2D-MIND/Ndc80c linkages (yellow)**, **Cse4-NCP/OA/2D-MIND/Ndc80c/Dam1c linkages (blue)**, and **Cse4-NCP/CI/ Mif2/ OA/ 2D-MIND/Ndc80c/Dam1c linkages (pink)**. The dashed horizontal line indicates 50% survival (median rupture force).

2.4 Discussion

We have reconstituted kinetochore assemblies capable of transmitting piconewton-scale forces from dynamic microtubules to Cse4-containing nucleosomes (**Figure 2-5**). To our knowledge, these are the most complete kinetochore assemblies made from individually purified *S. cerevisiae* components, representing the first reconstitution of the kinetochore's most basic

function: coupling centromeric nucleosomes to dynamic microtubule tips under physiologically relevant loads.

The self-assembly of kinetochore proteins at nanomolar concentrations strongly suggests that full-length kinetochore subcomplexes have much greater affinities for one another than suggested by the μM dissociation constants obtained using short peptides, probably because of additional points of contact [99,107,108]. We also demonstrate that there are two distinct and essential paths of force transmission through the inner kinetochore. Both OA and Mif2 are individually capable of forming load-bearing interactions with MIND. However, these paths are not equivalent. They are differentially sensitive to regulation by the major mitotic kinase, Ipl1 (Aurora B in humans), with the Mif2 path depending on the presence of phosphomimetic mutations on the MIND complex, whereas the OA pathway is only slightly strengthened by them. Also, while both the Mif2/2D-MIND and OA/2D-MIND interfaces are load-bearing, the former is mechanically weak relative to the Ndc80c/microtubule interface, but the latter is not (**Figure 2-4**).

We also found that OA can strengthen Mif2/2D-MIND/Ndc80c linkers, whereas Mif2 slightly weakens OA/2D-MIND/Ndc80c linkers. Although the '2D' phosphomimetic mutations on MIND partially alleviate autoinhibition, they do not abrogate it completely [99]. We speculate that OA binding to 2D-MIND alleviates this residual autoinhibition, promoting MIND's interaction with Mif2 and strengthening the Mif2-based chain. In contrast, in the OA-based linker, we hypothesize that OA disinhibition of 2D-MIND might permit Mif2 to outcompete OA for binding to 2D-MIND (**Figure 2-4**). In other words, Mif2 might decrease the rupture force of the OA/2D-MIND/Ndc80c linkers by "stealing" the disinhibited 2D-MIND from bead-bound OA, thus detaching MIND from the bead. Competition for binding to MIND is plausible, because previous work has shown that OA and Mif2 have directly adjacent binding sites on the same head of MIND [99].

When NCPs are on the bead, having both OA and Mif2 in solution strengthens the linkers (**Figure 2-5**). In this case OA and Mif2, which probably do not compete for binding to Cse4 [110,119,120,212], could each bind separate MIND complexes and thereby increase the total number of Ndc80c in the linker. Both OA and Mif2 exhibit a kinetochore function essential for genome stability: self-assembly exclusively on centromeric nucleosomes. Our kinetochore assemblies discriminate between NCPs that contain Cse4 and those that contain H3 (**Figure 2-5**). Yet we consistently find that Cse4 NCP-based chains are weak compared to shorter chains without

NCPs. We hypothesize that this relative weakness occurs because the Cse4 NCPs were wrapped in 601 DNA rather than centromeric DNA. Budding yeast Mif2 is reported to have a 40-fold greater affinity for Cse4-containing nucleosomes if they are wrapped in centromeric DNA [118]. We were unable to test the effect of this increased affinity on rupture force, because wrapping nucleosomes in centromeric DNA proved intractable.

Although both OA and Mif2 can both transmit force from Cse4 NCP to MIND, they are neither interchangeable nor redundant. There are several reasons that having multiple paths of force transmission might be advantageous. First, they can be regulated differently, which our data suggest is the case. Second, OA and Mif2 together increase the total number of outer kinetochore components that can be recruited. Estimates of the number of Ndc80 complexes present in each kinetochore vary from six to thirty copies [100,129,215], and biophysical experiments demonstrate that multiple Ndc80 complexes are necessary for effective microtubule coupling [88,92]. But MIND and Ndc80c interact in a 1:1 ratio [99,108], leading to the conclusion that the inner kinetochore must serve as an oligomerization platform, assembling on a single centromeric nucleosome and recruiting multiple copies of MIND and Ndc80c. If an OA complex and a Mif2 dimer assembled on each face of the centromeric nucleosome, they could collectively recruit up to 6 MIND/Ndc80c, with additional copies of Ndc80c potentially being recruited by the Cnn1 pathway [104].

Our findings also raise intriguing questions about how these multiple paths of force transmission and Ndc80c recruitment may be differentially utilized at different stages of the cell cycle or by different organisms. For instance, the human homolog of OA binds microtubules [111], but our finding that beads coated in OA do not bind microtubules in the absence of MIND (**Figure 2-3A**) makes it clear that budding yeast OA does not. For some organisms, OA is essential [201,216]; other species appear to lack OA homologs [122,123]. A smaller subset of organisms has no known homolog of Mif2 [123,128]. This strongly suggests that the relative importance of the OA and Mif2 pathways varies between organisms. There is also strong evidence for a third pathway of Ndc80c recruitment, through Cnn1 [104,217,218]. Although Cnn1 is not essential in yeast [77,219], it appears to play an important role in several other organisms [218,220,221]. Thus, while the branched architecture of the inner kinetochore is a feature conserved across many species, the relative importance of particular branches apparently varies between species

Taken together, our work represents a major advance towards the goal of reconstituting a complete, functional kinetochore from purely recombinant proteins. Going forward, the reconstituted "skeleton" kinetochore presented here can be used as a scaffold to study the contributions of other kinetochore proteins to force transmission. Of particular interest are Cnn1, which could increase rupture force by recruiting additional copies of Ndc80c [104,222], and Stu2, which is known to contribute significantly to kinetochore-microtubule coupling [200].

2.5 Acknowledgements

I thank Stephen Hinshaw (Harrison Lab, HMS) for a generous gift of Chl4/Iml3 expression vector pSMH104 and David Migl (Harrison Lab, HMS) for a generous gift of purified H3-H2A-H2B-H4 histone octamer. I also thank Michael Riffle for assistance with data analysis and visualization.

The research was supported by NIH grants R01 GM040506 and R35 GM130293 (TND), R01 GM079373 and R35 GM134842 (CLA), and NIH Training Grant in Molecular Biophysics T32 GM008268 (GEH).

YND and CN are employees at Genentech, Inc.

3 CHARACTERIZATION OF INTERACTIONS BETWEEN OA, MIF2, AND MIND

3.1 INTRODUCTION

Having demonstrated that both OA and Mif2 are capable of forming load-bearing attachments to MIND, I next asked whether they represent *independent* pathways of force transmission through the inner kinetochore. That is, do OA and Mif2 bind one another directly? Can they simultaneously bind to the same MIND complex?

Structural evidence obtained using *K.lactis* proteins and peptides suggests that OA and Mif2 bind noncompetitively to adjacent sites on the Mtw1/Nnf1 head of MIND [99]. And it has been reported, based on SEC co-elution experiments with *S. cerevisiae* OA, Mif2, and MIND, that all three form a co-complex containing multiple copies of each [107]. Interpretation of these data are complicated, however, by the fact that both OA and Mif2 are promiscuous DNA binders that co-purify with significant amounts of bacterial DNA when expressed recombinantly [107,114,118]. Indeed, the elution profile of the OA/Mif2/MIND co-complex observed by Hornung and coworkers was so extremely broad that they suggest "high-order associations" might be involved [107], as one might expect were Mif2 dimers effectively crosslinking pieces of bacterial DNA, some of which were also bound by OA.

In order to clarify the issue, my colleague and I purified OA and Mif2 under high-salt conditions that preclude co-purification of bacterial DNA (as determined by spectrophotometry and agarose gel electrophoresis). Using these purified proteins, we employed biochemical and biophysical techniques to explore the putative OA/Mif2/MIND interface.

3.2 PROTEIN CROSS-LINKING AND MASS-SPECTROMETRY

Intrigued by the different sensitivities of OA and Mif2 to autoinhibition within the MIND complex (**Figure 2-3** and **Figure 2-4**), we set to map these protein-protein interactions when autoinhibition within the MIND complex had been alleviated. We therefore mixed and cross-linked OA, Mif2, and 2D-MIND with the N-terminus of Dsn1 truncated ($Dsn1^{230-576}$-2D-MIND) in order to remove autoinhibition by this domain.

3.2.1 Methods

Cross-linking mass spectrometry (XL-MS) analysis was carried out as previously described [223]. Briefly, 100 µL final volume of a 1:1:1 mixture of OA, Mif2, and MIND was cross-linked at a final concentration of 1.5 µM per protein complex plus 0.49 mM DSS (disuccinimidyl suberate, Thermo Fisher Scientific cat. no. 21655) at room temperature in 30 mM HEPES buffer, pH 7.5, 150 mM NaCl, 1 mM TCEP. A 30 µL aliquot was removed after 5 minutes and the reaction quenched by addition of 3 µL 1 M ammonium bicarbonate. Cross-linked proteins were reduced with 5 mM TCEP in 0.1% PPS Silent® Surfactant (Expedeon cat. no. 21011) at 60°C for 1 h followed by alkylation with 6 mM iodoacetamide for 20 minutes at room temperature. Protein was digested with sequencing grade modified trypsin (Promega Corp. cat. no. V5111) at an enzyme:substrate ratio of 1:15 at 37°C for 4 h with shaking at 1200 rpm. After digestion samples were brought to 250 mM HCl and incubated for 1 h at room temperature before storage at -80°C. Liquid Chromatography Mass Spectrometry (LCMS) analysis was done using a 3 µL sample loaded onto a fused-silica capillary tip column (75-µm i.d.) packed with 30 cm of Reprosil-Pur C18-AQ (3-µm bead diameter, Dr. Maisch). An acetonitrile gradient was run at 0.25 µL/min to elute peptides into a QExactive HF mass spectrometer (Thermo Fisher Scientific). Spectra were collected in data dependent mode and converted into mzML using msconvert from ProteoWizard [224].

Cross-linked peptides were identified using the Kojak version 1.4.3 cross-link identification software [225] (www.kojak-ms.org) and Percolator version 2.08) [226] was used to produce a statistically validated set of cross-linked peptides. ProXL [227,228] (http://proxl-ms.org/) was used for analysis and visualization of cross-linked peptides.

3.2.2 Results and discussion

We observed numerous cross-links between the N-terminus of Mif2 and the Nnf1/Mtw1 head of MIND, as well as cross-links between the N-terminus of Ame1 and the Nnf1/Mtw1 head of MIND in agreement with previously reported interfaces (**Figure 3-1**) [99,107]. We also observed cross-links between MIND and regions of Mif2 beyond the first 40 residues, suggesting that the extreme N-terminus of Mif2 might not be the sole domain mediating Mif2/MIND interactions. This theory is supported by our finding that truncation of the first 40 amino acids of

Mif2 does not completely abrogate its interaction with MIND (**Figure 2-4**). Based on crosslinks between Mif2, Dsn1, and Nsl1, we speculate that Mif2 may actually interact with both heads of the Y-shaped MIND complex.

We did not, however, observe any crosslinks between OA and Mif2, as would normally be expected if the two complexes bound one another directly or if they simultaneously bound the same MIND complex at adjacent sites. While the absence of crosslinks cannot preclude interaction between two protein subcomplexes, these results suggest that OA and Mif2 might not bind one another directly or through MIND. In order to test this hypothesis, we turned to SEC with multi-angle light scattering (SEC-MALS).

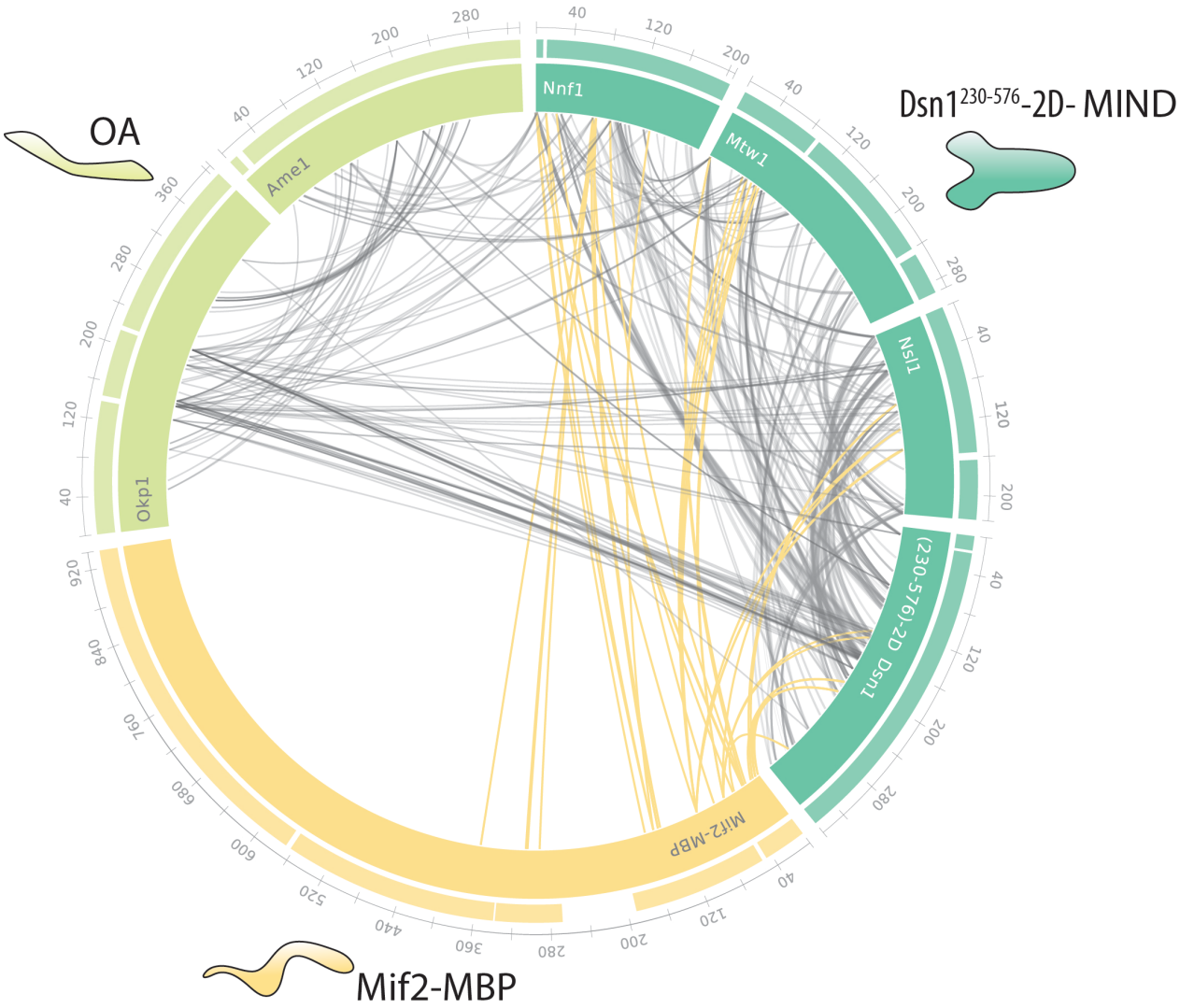

Figure 3-1. Circle-plot of cross-links obtained with co-incubated OA, Mif2, and Dsn1$^{230-576}$-2D-MIND using disuccinimidyl suberate (DSS). Cross-links between and within OA and Dsn1$^{230-576}$-2D-MIND complexes are shown as grey lines. Cross-links between Mif2 and Dsn1$^{230-576}$-2D-MIND complexes are shown as yellow lines. The outermost ring of the circle indicates sequence coverage, corresponding to 88% for Mif2, 97% for OA and 95% for Dsn1$^{230-576}$-2D-MIND.

3.3 SIZE-EXCLUSION CHROMATOGRAPHY AND MULTI-ANGLE LIGHT SCATTERING (SEC-MALS)

In order to determine whether or not purified OA, Mif2, and MIND do indeed form a co-complex in the absence of DNA, we decided to analyze these protein subcomplexes individually and in combination using SEC-MALS.

A truncated and phosphomimetic MIND construct (Dsn1$^{230\text{-}576}$-2D-MIND) was used in order to minimize both sample heterogeneity and autoinhibition. Dsn1$^{230\text{-}576}$-2D-MIND behaved exclusively as a monomer (**Figure 3-2**). A minor population of recombinant MIND dimers has been reported at high concentrations (> 10 mg/mL) [99], but it was neither expected nor observed at the much lower concentrations that we tested.

OA exhibited an average molecular mass of about 110 kDa, in between the values expected for a monomer and a dimer (**Figure 3-2**). This indicates a monomer/dimer equilibrium [229]. I speculate that, in the absence of Nkp1/Nkp2, contacts that are normally made between the two heterodimers are left unsatisfied, causing OA to form transient, non-native dimers.

Mif2-MBP was by far the most poorly behaved of the protein subcomplexes, exhibiting molecular masses significantly higher than expected for a dimer (**Figure 3-2**). The broad, asymmetrical Mif2-MBP elution peak had a pronounced right tail, likely containing products of the degradation of the N-terminus of Mif2, which are always visible on SDS-PAGE gels. Except for its cupin fold, Mif2 is largely disordered [114,115], which may contribute to its heterogeneous behavior. Because we were unable to determine the baseline oligomeric state of Mif2-MBP in solution, no further SEC-MALS experiments were conducted using Mif2.

Instead OA and Dsn1$^{230\text{-}576}$-2D-MIND were combined in a 2:1 ratio, and two elution peaks were observed (**Figure 3-2**). One had a molecular weight of 412 kDa, very close to the 420 kDa predicted for a 2:2 OA/MIND co-complex. The molecular weight of the second peak (311 kDa) is close to the predicted weight a 2:1 OA/MIND co-complex (296 kDa). This suggests that dimeric species of OA persist after binding MIND.

In the future, SEC-MALS will be used to determine if the monomer-dimer equilibrium of OA in solution persists in the presence of its binding partner, Nkp1/Nkp2. If OA and Nkp1/Nkp2 form a stable, monomeric heterotetramer, it would support the suggestions that these four proteins constitute conserved a “NANO” subcomplex [76,124].

We will also attempt SEC-MALS analysis of a truncated Mif2 construct lacking its DNA-binding and dimerization domains. If this construct behaves more homogenously than full-length Mif2, then it could be used to verify the existence of OA/Mif2/MIND co-complexes and define their stoichiometry.

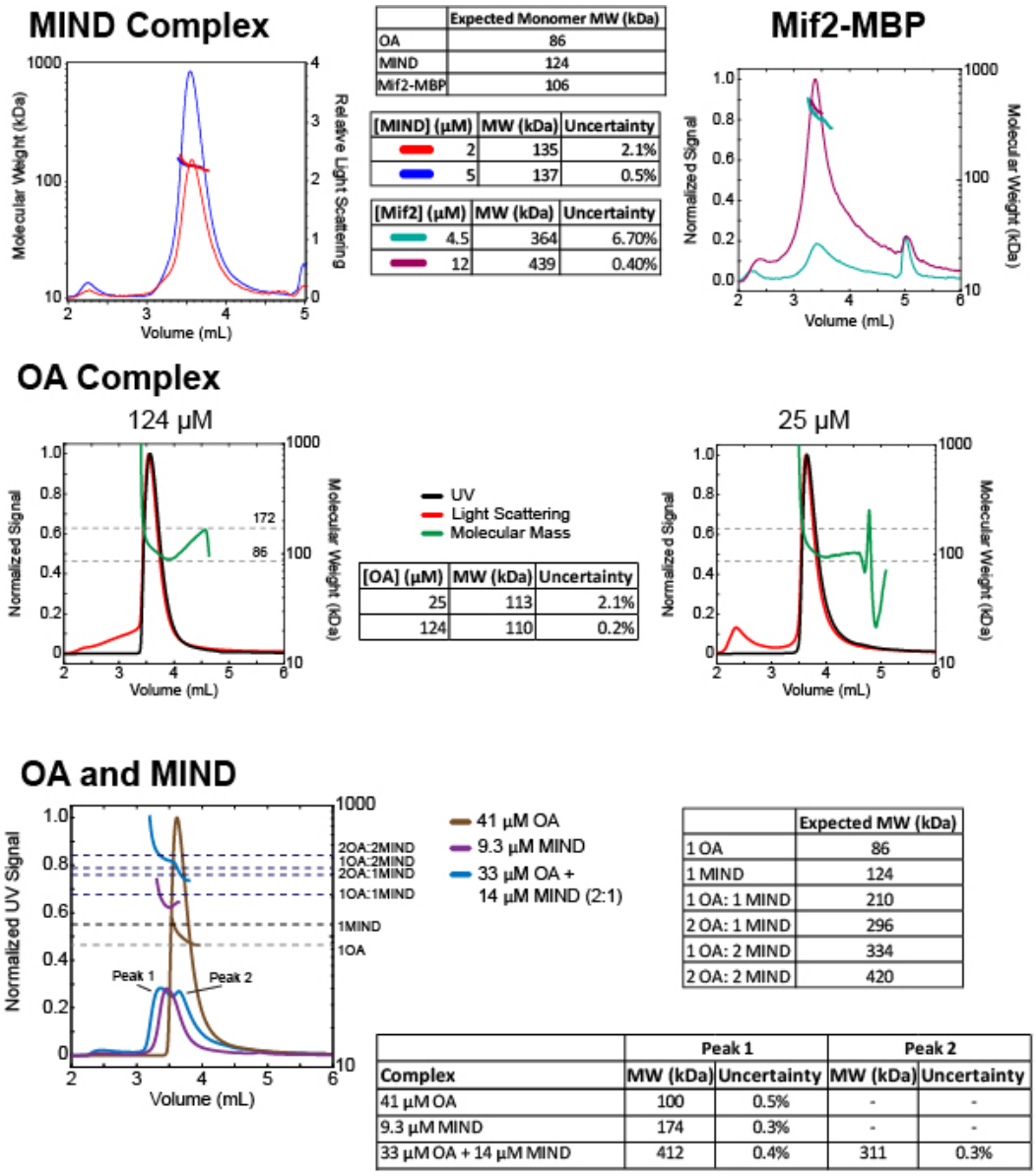

	Expected Monomer MW (kDa)
OA	86
MIND	124
Mif2-MBP	106

[MIND] (µM)	MW (kDa)	Uncertainty
2	135	2.1%
5	137	0.5%

[Mif2] (µM)	MW (kDa)	Uncertainty
4.5	364	6.70%
12	439	0.40%

[OA] (µM)	MW (kDa)	Uncertainty
25	113	2.1%
124	110	0.2%

	Expected MW (kDa)
1 OA	86
1 MIND	124
1 OA: 1 MIND	210
2 OA: 1 MIND	296
1 OA: 2 MIND	334
2 OA: 2 MIND	420

	Peak 1		Peak 2	
Complex	MW (kDa)	Uncertainty	MW (kDa)	Uncertainty
41 µM OA	100	0.5%	-	-
9.3 µM MIND	174	0.3%	-	-
33 µM OA + 14 µM MIND	412	0.4%	311	0.3%

Figure 3-2. SEC-MALS analysis of MIND, OA, Mif2, and an OA/MIND co-complex.

3.4 SINGLE-MOLECULE TOTAL INTERNAL REFLECTION FLUORESCENCE (SMTIRF) MICROSCOPY

Because SEC-MALS and protein cross-linking mass spectrometry, both bulk assaysyielded equivocal results, we designed a single-molecule TIRF (smTIRF) assay in order to determine if OA and Mif2 could simultaneously bind to the same MIND complex. Briefly, glass slides and functionalized coverslips were used to construct flow chambers, as reported previously [90,191]. Full-length GFP-labeled 2D-MIND complexes were specifically adhered to coverslip surfaces. OA labeled with Alexa Fluor® 546 and Mif2 labeled with Alexa Fluor® 647 were flowed into the chamber. Unbound OA and Mif2 were then washed out. Using three-color TIRF microscopy, the MIND complexes that formed co-complexes with Mif2 and/or OA were distinguished from those that did not by assessing colocalization of the GFP signal with Alexa Fluor® 546 and Alexa Fluor® 647 dyes (**Figure 3-3**).

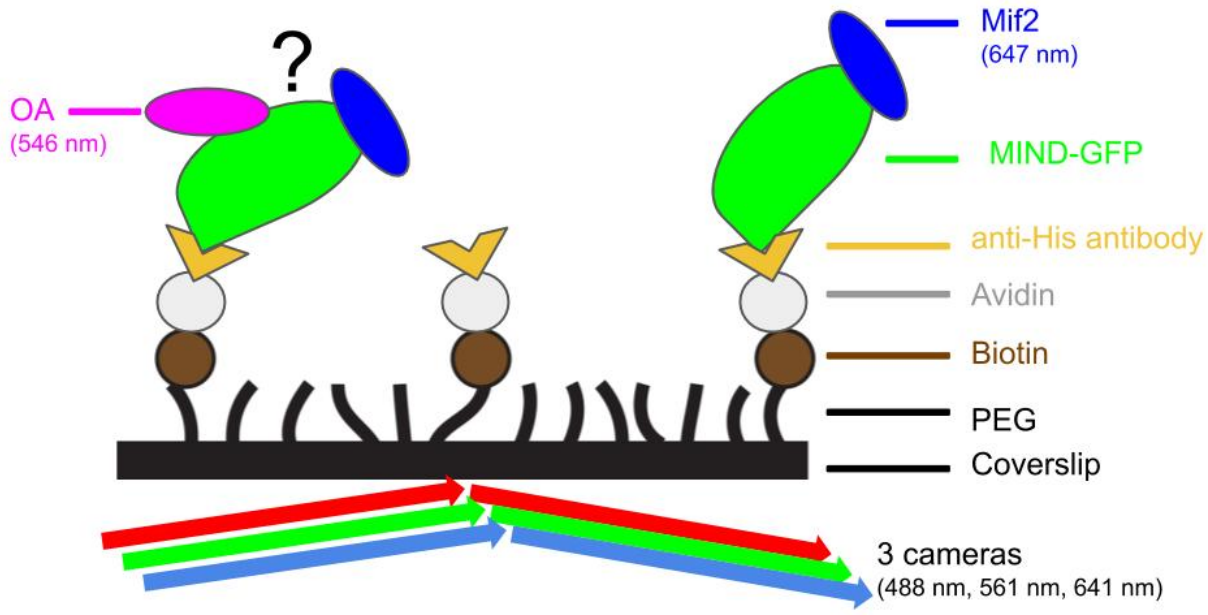

Figure 3-3. Schematic of smTIRF assay.

We observed both OA/2D-MIND and Mif2/2D-MIND colocalization events, as well as much rarer triple colocalization events (**Figure 3-4**). Although less than 1% of 2D-MIND molecules colocalized with both OA and Mif2, it is tempting to conclude that OA and Mif2 *can* bind the same 2D-MIND simultaneously but do so only rarely. Intensity profiles suggest single

2D-MIND molecules are present in the triple colocalization, meaning the OA and Mif2 are not merely binding to adjacent 2D-MIND molecules. However, we also observed OA and Mif2 colocalization in the absence of 2D-MIND. This suggests that either some fraction of the GFP tags on MIND were non-fluorescent or Mif2 and OA absorbed non-specifically to the coverslip. Thus, it is possible that incomplete passivation of the coverslip could be responsible for some of the triple colocalization events.

A further caveat: while there is certainly much less co-purifying DNA when OA and Mif2 are purified under high-salt conditions, we cannot preclude that some very small amount of DNA (undetectable by agarose gel electrophoresis) remains. This complicates interpretation of data from this single-molecule assay, as only a very small number of triple colocalization events were observed.

					BINDING EVENTS				FALSE POSITIVES			% Events that maybe False		
Date	Reaction	# of MINDs	# of OAs	# of Mif2s	OA-MIND	Mif2-MIND	OA-Mif2-MIND	% Mif2s have OA	OA-MIND	Mif2-MIND	OA-Mif2-MIND	OA-MIND	Mif2-MIND	OA-Mif2-MIND
12/4	1nM MIND + 0.2nM Mif2 + 0.2nM OA	32003	10531	5995	3467	1014	291	28.7%	115	67	1	3.32%	6.61%	0.34%
12/4	1nM MIND + 0.2nM Mif2 + 0.2nM OA	9781	4335	3213	665	113	35	31.0%	15	12	0	2.26%	10.62%	0.00%

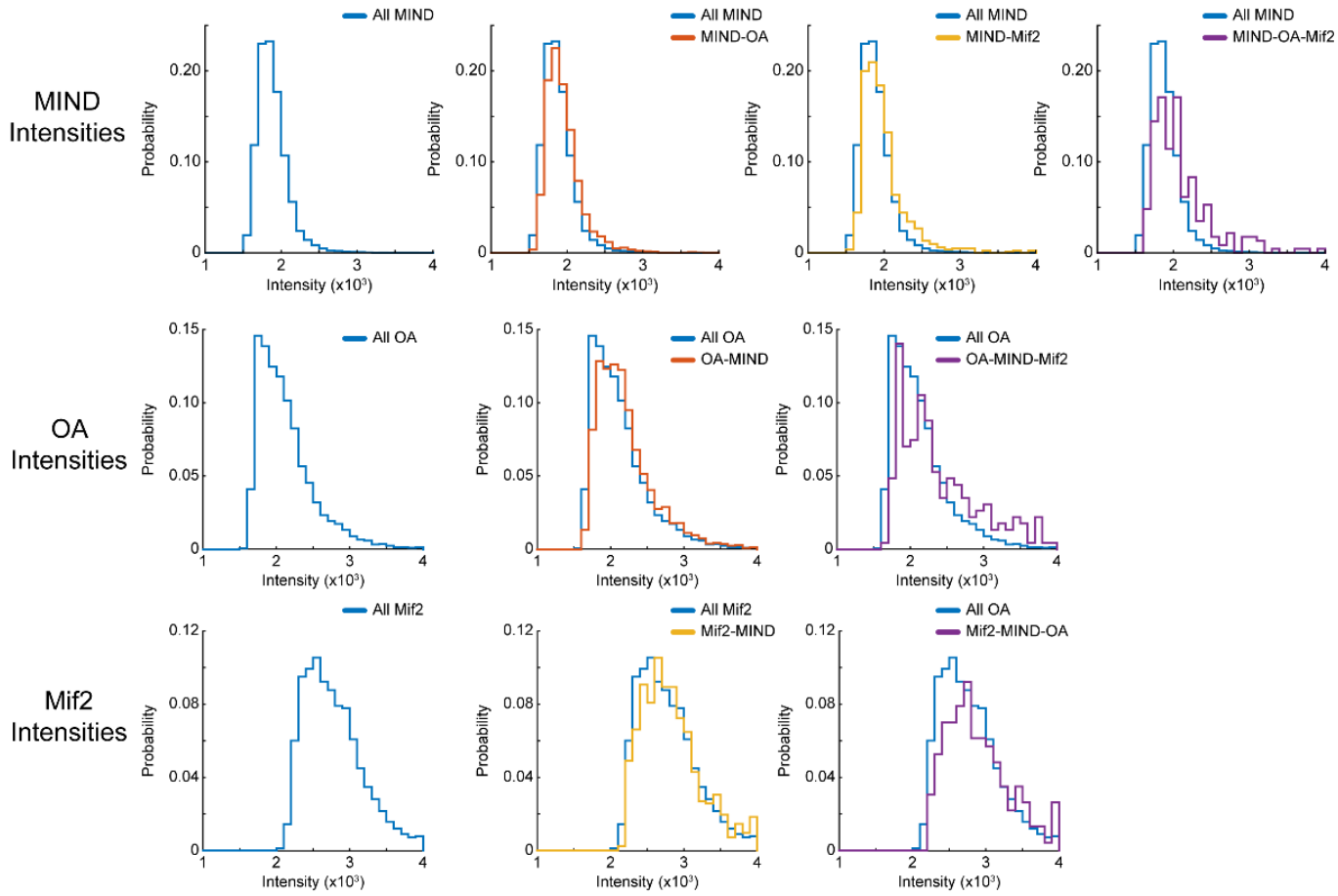

Figure 3-4. TIRF-based assay reveals rare triple colocalization of individual molecules of OA, Mif2, and 2D-MIND.

Based on this assay, we can neither confirm nor deny that OA and Mif2 are capable of binding to the same MIND complex simultaneously, but smTIRF experiments have been informative in other ways. For instance, intensity profiles suggest that many OA molecules may be dimers, in agreement with our SEC-MALS data (**Figure 3-2**). Intriguingly, while 7.9% of the OA/2D-MIND colocalization events also had a colocalized Mif2, 29% of the Mif2/2D-MIND colocalization events also had a colocalized OA. This could suggest that OA binding alleviates remaining autoinhibition within 2D-MIND (the two phosphomimetic mutations do not completely abrogate autoinhibition [99]), allowing Mif2 to bind. That would also explain how OA strengthens Mif2/2D-MIND/Ndc80c chains in our rupture force assay (**Figure 2-4B and C**).

Although it could not answer the question of whether or not OA and Mif2 bind the same MIND simultaneously, the smTIRF assay will be a useful tool for exploring how the OA/MIND and Mif2/MIND interfaces are regulated. For instance, by tethering different GFP-tagged MIND constructs to the coverslip, we can compare lifetimes of attachment from OA and Mif2 to wild-type and phosphomimetic MIND and determine how much of Dsn1 must be truncated in order to completely abrogate autoinhibition within the MIND complex.

3.5 Discussion

Just as in previous studies [107], all of my experimental results have been equivocal when it comes to binding between *S. cerevisiae* OA and Mif2 in the presence or absence of MIND. Unequivocal evidence for or against such interactions has also eluded scientists working with *K. lactis* OA and Mif2 (Yoana Dimitrova, personal communication). I therefore hypothesize that previously reported promiscuous DNA-binding by both Mif2 and OA can cause these two protein complexes to co-elute [107], despite the lack of direct association. An alternative explanation is that Mif2 and OA do associate directly, but only when the former has PTMs; the Mif2 used by Hornung and coworkers to identify direct binding was recombinantly purified from insect cells [107], whereas we express Mif2 in *E. coli*.

But our failure to observe either direct OA/Mif2 binding or unequivocal evidence of *in*direct binding through MIND cannot preclude the possibility that such interactions exist under conditions other than those tested. Further experimentation will be necessary to answer this question. If, for example, the addition of DNAse to the smTIRF flow chamber decreased the incidence of triple colocalization events, then it would suggest that these events were the result of promiscuous DNA binding rather than true OA/Mif2/MIND co-complexes.

3.6 Acknowledgements

Thanks to Alex Zelter, Evie Henry, and Michael MacCoss for protein cross-linking mass spectrometry experiments and analysis. Tremendous thanks to Luke Helgeson for SEC-MALS and smTIRF experiments, data analysis, and visualization.

4 CONCLUSIONS

We have reconstituted, from individually purified components, the kinetochore's most basic function: coupling centromeric nucleosomes to dynamic microtubule tips under load. We report self-assembly at nanomolar concentrations of the most complete kinetochore assemblies ever reconstituted from *S. cerevisiae* proteins. We also demonstrate that there are two distinct and essential paths of force transmission through the inner kinetochore and that these two paths, through OA and Mif2, are differentially sensitive to regulation by the major mitotic kinase, Ipl1.

At every step of the effort to reconstitute functional kinetochores, we find that this remarkable molecular machine is more than the sum of its parts. A single Ndc80c molecule is incapable of coupling to dynamic microtubules [88,92]. Multiple copies of Ndc80c, while capable of microtubule coupling, function much more robustly in tandem with Dam1c [87-93]. And MIND, while not itself a microtubule binder, improves the microtubule coupling ability of Ndc80c by promoting its extended, uninhibited conformation [86,98]. This trend continues into the inner kinetochore. OA/2D-MIND/Ndc80c chains and Mif2/2D-MIND/Ndc80c chains are both mechanically stronger than 2D-MIND/Ndc80c chains (**Figure 2-3** and **Figure 2-4**). And NCP-based chains containing both OA and Mif2 are stronger than chains containing either alone (**Figure 2-5**).

But because both OA and Mif2 are individually capable of forming load-bearing interactions with MIND and Cse4, they represent two potentially distinct means of transmitting force from the outer kinetochore to the centromere. This work raises questions about the functional architecture of the inner kinetochore, Ipl1 regulation of kinetochore assembly and disassembly, and the remarkable ability of the kinetochore to self-assemble *in vitro*.

4.1 KINETOCHORE AS SELF-ASSEMBLING MACHINE

Intermolecular self-assembly at nanomolar concentrations is no mean feat. It has been described in few other biological systems. Microtubules self-assemble from tubulin dimers *in vitro* only above a critical threshold concentration of about 14 μM, or as little as 2 μM if templated [28,230,231]. Viral capsid proteins have been observed self-assembling at concentrations as low as 0.44 μM [232]. While double-stranded DNA molecules can self-assemble at nanomolar concentrations [233], it can be difficult to monitor protein behavior at such low concentrations,

and it was only thanks to our powerful optical trap-based functional assay that we were able to do so. Our finding that kinetochore protein subcomplexes self-assemble into functional microtubules couplers *in vitro* at 10-nM concentrations has several major implications.

The deposition and maintenance of centromeric nucleosomes is tightly regulated [138,140,234]. Because the kinetochore discriminates exquisitely between centromeric and non-centromeric nucleosomes (**Figure 2-5A**)[118,235], perhaps kinetochore assembly does not require the same level of regulatory supervision.

The vast majority of PTMs of kinetochore proteins weaken their interactions with each other and with microtubules [94,110,236-238]. A general trend emerges: the kinetochore can spontaneously self-assemble at extraordinarily low concentrations without the help of any kinases, which mainly function in prompting kinetochore *disassembly* as a means of error correction. But this trend has one major exception: we found that two specific PTM-mimicking mutations actually promote the kinetochore's remarkable feat of self-assembly.

4.2 IPL1 REGULATION OF KINETOCHORE ASSEMBLY AND DISASSEMBLY

We report that OA and Mif2 are differentially sensitive to phosphorylation of MIND component Dsn1 by Ipl1 (**Figure 2-3** and **Figure 2-4**). While phosphomimetic mutations to Dsn1 increased the strength of OA-MIND interactions, they were actually *necessary* for robust Mif2/MIND interaction. What does it mean that phosphorylation by Ipl1, which weakens kinetochore-microtubule attachment in the outer kinetochore [239], is necessary for full-strength interactions between MIND and its inner kinetochore binding partners?

A master mitotic regulator, Ipl1 has been the subject of intense study and debate. $Sli15^{INCEP}$, $Bir1^{Survivin}$, $Nbl1^{Borealin}$, and $Ipl1^{Aurora\ B}$ make up the conserved chromosomal passenger complex (CPC), which localizes to different parts of the mitotic spindle in distinct ways. The centromeric CPC pool is recruited through interactions between Bir1 and Ndc10 or phosphorylated histone H2A [240]. Ipl1 is most enriched at the centromere from prophase to metaphase, and at anaphase onset it relocalizes to the spindle midzone [241]. The CPC can also bind directly to microtubules [242,243], creating a microtubule-associated CPC pool. There is also an inner kinetochore associated pool of CPC, created by the physical interaction between Sli15 and Ctf19 [109,244].

Which of these three CPC pools is responsible for phosphorylation of Dsn1 and thus regulation of the MIND/inner kinetochore interface? The answer has implications for conflicting models of Ipl1$^{\text{Aurora B}}$ function in error correction.

The once-dominant spatial signaling model posits that the centromere-associated CPC pool creates a gradient of Ipl1$^{\text{Aurora B}}$ activity, greatest at the centromere and weaker at the outer kinetochore, which is pulled out of range by tension. When a misaligned kinetochore is not under tension, the kinetochore shortens, bringing outer kinetochore substrates into range of centromere-associated Ipl1$^{\text{Aurora B}}$, causing detachment from the improperly attached microtubule [245,246]. Several findings have challenged this model: (1) Bir1, which mediates CPC localization to the centromere, is inessential for both viability and kinetochore biorientation in budding yeast [247], as is the chromatin-targeting domain of Sli15 [248]; (2) Ectopic targeting of Ipl1$^{\text{Aurora B}}$ to the kinetochore does not, by itself, cause kinetochore detachment [96]; (3) A subpopulation of Ipl1$^{\text{Aurora B}}$ remains localized at the outer kinetochore even after its substrate, Ndc80$^{\text{Hec1}}$, is dephosphorylated, and Ndc80$^{\text{Hec1}}$ is not highly re-phosphorylated in response to loss of tension [236]. Taken together, these results cast doubt on the model of error correction mediated by spatial positioning of Ipl1$^{\text{Aurora B}}$.

A recently proposed alternative model posits that the centromere-associated CPC pool functions primarily in protecting sister chromatid cohesion, while the microtubule-associated CPC pool mediates error correction by tuning kinetochore-microtubule attachment strength [241,247,248]. Further evidence from human and chicken cell lines supports the notion that the centromere-associated CPC pool is dispensable for error correction [249-251].

Bonner and colleagues report that, in *Xenopus* egg extracts, localization of Ipl1$^{\text{Aurora B}}$ to the inner kinetochore is essential for Dsn1 phosphorylation, and that transient interactions with Mif2$^{\text{CENP-C}}$ promote phosphorylation of the N-terminus of Dsn1 [252]. I hypothesize that in budding yeast OA, which we found to be less sensitive to the phosphorylation state of Dsn1 (**Figure 2-3** and **Figure 2-4**), could initially interact with MIND, displacing the autoinhibitory tail and making it accessible to phosphorylation by inner kinetochore-localized Ipl1$^{\text{Aurora B}}$. If my hypothesis that OA/MIND interactions license Mif2/MIND interactions is correct, it could explain why the MIND-binding N-terminus of Ame1 is essential for viability, while the primary MIND-binding domain of Mif2 is not [107] and our preliminary finding that many Mif2/MIND interactions also had a colocalized OA (**Figure 3-4**).

In summary, it seems likely that the inner kinetochore-associated CPC pool responsible for regulating inner kinetochore assembly is independent from both the centromere-associated CPC pool and the microtubule-associated CPC pool that mediates error correction.

4.3 FUNCTIONAL ARCHITECTURE OF THE INNER KINETOCHORE.

We demonstrated that there are two essential paths of force transmission through the inner kinetochore: OA and Mif2. Why are there at least two distinct means of transmitting force from the outer kinetochore to the centromere? Presumably this organization increases the total number of outer kinetochore components that can be recruited, but are the means of recruitment functionally different? That the MIND-binding domain of OA— but not the primary MIND binding domain of Mif2— is essential suggests that this may be the case [107]. And if MIND recruitment is not Mif2's essential function, what is?

OA and Mif2 are the sole essential components of the budding yeast inner kinetochore. Our finding that both are independently capable of transmitting force through from MIND to the centromeric nucleosome raises the question: do inessential inner kinetochore protein subcomplexes contribute anything to that endeavor? Recent structural work suggests that OA is intimately associated with the Nkp1 and Nkp2 [103,124]. The organization of the four proteins resembles that of the MIND complex, with extensive contacts between two coiled coils [76,99,103]. Although OA and NN can be expressed and purified independently, and although the former is essential and the latter is not, together they may represent a conserved protein subcomplex. Multiple studies have found negative genetic interactions between Nkp1/Nkp2 and OA [253,254]. And although *nkp1* and *nkp2* are both inessential, deletion of either gene is synthetic lethal with the *okp1-5* temperature-sensitive allele [255].

I propose that the true test of whether or not Nkp1/Nkp2 and OA should be considered members of the same subcomplex is if Nkp1/Nkp2 contributes to the biochemical and mechanical functions of OA. That is, does formation of a NANO tetramer affect OA dimerization? Does it alter the binding dynamics or mechanical strength of OA/MIND or OA/Cse4 interactions? Using recombinantly expressed and purified Nkp1/Nkp2 and the same biophysical assays that have already been used to describe OA alone, I hope to answer these questions imminently.

Another potential contributor to robust centromeric nucleosome attachment is the DNA-binding subcomplex Chl4/Iml3. Although adding CI in solution did not significantly strengthen

Cse4 NCP-based chains containing both OA and Mif2 (**Figure 2-6**), a recent structure of the inner kinetochore in association with a centromeric nucleosome suggests that Ctf19/Mcm21 connects CI to OA [124]. I speculate that the addition of CI *and* Ctf19/Mcm21 could mechanically strengthen the interaction between OA and centromeric nucleosomes, a hypothesis that can be readily tested using our optical trap rupture force assay.

In summary, using the biophysical assays and biochemical reconstitution efforts that have been decades in the making, we are finally poised to understand how the kinetochore functions as a whole greater than the sum of its many parts.

BIBLIOGRAPHY

1. Boveri T: **Ueber mehrpolige Mitosen als Mittel zur Analyse des Zellkerns**. Edited by: Verh Phys-med Ges Würzburg NF. ; 1902:67-90. vol 35.]
2. Stingele S, Stoehr G, Peplowska K, Cox J, Mann M, Storchova Z: **Global analysis of genome, transcriptome and proteome reveals the response to aneuploidy in human cells**. *Mol Syst Biol* 2012, **8**:608.
3. Upender MB, Habermann JK, McShane LM, Korn EL, Barrett JC, Difilippantonio MJ, Ried T: **Chromosome transfer induced aneuploidy results in complex dysregulation of the cellular transcriptome in immortalized and cancer cells**. *Cancer Res* 2004, **64**:6941-6949.
4. Torres EM, Sokolsky T, Tucker CM, Chan LY, Boselli M, Dunham MJ, Amon A: **Effects of aneuploidy on cellular physiology and cell division in haploid yeast**. *Science* 2007, **317**:916-924.
5. Oromendia AB, Dodgson SE, Amon A: **Aneuploidy causes proteotoxic stress in yeast**. *Genes Dev* 2012, **26**:2696-2708.
6. Tsai HJ, Nelliat AR, Choudhury MI, Kucharavy A, Bradford WD, Cook ME, Kim J, Mair DB, Sun SX, Schatz MC, et al.: **Hypo-osmotic-like stress underlies general cellular defects of aneuploidy**. *Nature* 2019, **570**:117-121.
7. de Wolf B, Kops G: **Kinetochore Malfunction in Human Pathologies**. *Adv Exp Med Biol* 2017, **1002**:69-91.
8. Li TC, Makris M, Tomsu M, Tuckerman E, Laird S: **Recurrent miscarriage: aetiology, management and prognosis**. *Hum Reprod Update* 2002, **8**:463-481.
9. Ganmore I, Smooha G, Izraeli S: **Constitutional aneuploidy and cancer predisposition**. *Hum Mol Genet* 2009, **18**:R84-93.
10. Beroukhim R, Mermel CH, Porter D, Wei G, Raychaudhuri S, Donovan J, Barretina J, Boehm JS, Dobson J, Urashima M, et al.: **The landscape of somatic copy-number alteration across human cancers**. *Nature* 2010, **463**:899-905.
11. Lengauer C, Kinzler KW, Vogelstein B: **Genetic instability in colorectal cancers**. *Nature* 1997, **386**:623-627.
12. Giam M, Rancati G: **Aneuploidy and chromosomal instability in cancer: a jackpot to chaos**. *Cell Div* 2015, **10**:3.
13. Davoli T, Xu AW, Mengwasser KE, Sack LM, Yoon JC, Park PJ, Elledge SJ: **Cumulative haploinsufficiency and triplosensitivity drive aneuploidy patterns and shape the cancer genome**. *Cell* 2013, **155**:948-962.
14. Santaguida S, Amon A: **Short- and long-term effects of chromosome mis-segregation and aneuploidy**. *Nat Rev Mol Cell Biol* 2015, **16**:473-485.
15. Roschke AV, Rozenblum E: **Multi-layered cancer chromosomal instability phenotype**. *Front Oncol* 2013, **3**:302.
16. Remak R: **Untersuchungen über die Entwickelung der Wirbelthiere**. Edited by. Berlin: G. Reimer; 1855.
17. Paweletz N: **Walther Flemming: pioneer of mitosis research**. *Nat Rev Mol Cell Biol* 2001, **2**:72-75.
18. Flemming W: **Zellsubstanz, Kern und Zelltheilung**. Edited by. Leipzig: F. C. W. Vogel; 1882.
19. Inoué S: **Polarization optical studies of the mitotic spindle. I. The demonstration of spindle fibers in living cells**. *Chromosoma* 1953, **5**:487-500.
20. Ito D, Bettencourt-Dias M: **Centrosome Remodelling in Evolution**. *Cells* 2018, **7**.
21. Powell MJ: **Mitosis in the aquatic fungus Rhizophydium spherotheca**. *American Journal of Botany* 1980, **67**:839-853.
22. Moens PB, Rapport E: **Spindles, spindle plaques, and meiosis in the yeast Saccharomyces cerevisiae (Hansen)**. *J Cell Biol* 1971, **50**:344-361.
23. Geissler S, Pereira G, Spang A, Knop M, Soues S, Kilmartin J, Schiebel E: **The spindle pole body component Spc98p interacts with the gamma-tubulin-like Tub4p of Saccharomyces cerevisiae at the sites of microtubule attachment**. *Embo j* 1996, **15**:3899-3911.
24. Kollman JM, Polka JK, Zelter A, Davis TN, Agard DA: **Microtubule nucleating gamma-TuSC assembles structures with 13-fold microtubule-like symmetry**. *Nature* 2010, **466**:879-882.
25. O'Toole ET, Winey M, McIntosh JR: **High-voltage electron tomography of spindle pole bodies and early mitotic spindles in the yeast Saccharomyces cerevisiae**. *Mol Biol Cell* 1999, **10**:2017-2031.
26. Nogales E, Whittaker M, Milligan RA, Downing KH: **High-resolution model of the microtubule**. *Cell* 1999, **96**:79-88.
27. Chaaban S, Brouhard GJ: **A microtubule bestiary: structural diversity in tubulin polymers**. *Mol Biol Cell* 2017, **28**:2924-2931.
28. Mitchison T, Kirschner M: **Microtubule assembly nucleated by isolated centrosomes**. *Nature* 1984, **312**:232-237.
29. Mitchison T, Kirschner M: **Dynamic instability of microtubule growth**. *Nature* 1984, **312**:237-242.
30. Kobayashi T: **Dephosphorylation of tubulin-bound guanosine triphosphate during microtubule assembly**. *J Biochem* 1975, **77**:1193-1197.
31. Alushin GM, Lander GC, Kellogg EH, Zhang R, Baker D, Nogales E: **High-resolution microtubule structures reveal the structural transitions in alphabeta-tubulin upon GTP hydrolysis**. *Cell* 2014, **157**:1117-1129.
32. Mandelkow EM, Mandelkow E, Milligan RA: **Microtubule dynamics and microtubule caps: a time-resolved cryo-electron microscopy study**. *J Cell Biol* 1991, **114**:977-991.
33. Inoue S, Sato H: **Cell motility by labile association of molecules. The nature of mitotic spindle fibers and their role in chromosome movement**. *J Gen Physiol* 1967, **50**:Suppl:259-292.
34. Driver JW, Geyer EA, Bailey ME, Rice LM, Asbury CL: **Direct measurement of conformational strain energy in protofilaments curling outward from disassembling microtubule tips**. *Elife* 2017, **6**.
35. Inoué S, Salmon ED: **Force generation by microtubule assembly/disassembly in mitosis and related movements**. *Mol Biol Cell* 1995, **6**:1619-1640.
36. Desai A, Mitchison TJ: **Microtubule polymerization dynamics**. *Annu Rev Cell Dev Biol* 1997, **13**:83-117.
37. McIntosh JR, Volkov V, Ataullakhanov FI, Grishchuk EL: **Tubulin depolymerization may be an ancient biological motor**. *J Cell Sci* 2010, **123**:3425-3434.
38. Mandrioli M, Manicardi GC: **Unlocking holocentric chromosomes: new perspectives from comparative and functional genomics?** *Curr Genomics* 2012, **13**:343-349.
39. Marques A, Pedrosa-Harand A: **Holocentromere identity: from the typical mitotic linear structure to the great plasticity of meiotic holocentromeres**. *Chromosoma* 2016, **125**:669-681.
40. Allshire RC, Karpen GH: **Epigenetic regulation of centromeric chromatin: old dogs, new tricks?** *Nat Rev Genet* 2008, **9**:923-937.
41. Murillo-Pineda M, Jansen LET: **Genetics, epigenetics and back again: Lessons learned from neocentromeres**. *Exp Cell Res* 2020:111909.

42. Clarke L, Carbon J: **Isolation of a yeast centromere and construction of functional small circular chromosomes**. *Nature* 1980, **287**:504-509.
43. Clarke L, Carbon J: **The structure and function of yeast centromeres**. *Annu Rev Genet* 1985, **19**:29-55.
44. Wiens GR, Sorger PK: **Centromeric chromatin and epigenetic effects in kinetochore assembly**. *Cell* 1998, **93**:313-316.
45. Henikoff S, Furuyama T: **Epigenetic inheritance of centromeres**. *Cold Spring Harb Symp Quant Biol* 2010, **75**:51-60.
46. Earnshaw WC, Rothfield N: **Identification of a family of human centromere proteins using autoimmune sera from patients with scleroderma**. *Chromosoma* 1985, **91**:313-321.
47. Keith KC, Baker RE, Chen Y, Harris K, Stoler S, Fitzgerald-Hayes M: **Analysis of primary structural determinants that distinguish the centromere-specific function of histone variant Cse4p from histone H3**. *Mol Cell Biol* 1999, **19**:6130-6139.
48. Black BE, Jansen LE, Maddox PS, Foltz DR, Desai AB, Shah JV, Cleveland DW: **Centromere identity maintained by nucleosomes assembled with histone H3 containing the CENP-A targeting domain**. *Mol Cell* 2007, **25**:309-322.
49. French BT, Westhorpe FG, Limouse C, Straight AF: **Xenopus laevis M18BP1 Directly Binds Existing CENP-A Nucleosomes to Promote Centromeric Chromatin Assembly**. *Dev Cell* 2017, **42**:190-199.e110.
50. Hori T, Shang WH, Hara M, Ariyoshi M, Arimura Y, Fujita R, Kurumizaka H, Fukagawa T: **Association of M18BP1/KNL2 with CENP-A Nucleosome Is Essential for Centromere Formation in Non-mammalian Vertebrates**. *Dev Cell* 2017, **42**:181-189.e183.
51. Zasadzinska E, Huang J, Bailey AO, Guo LY, Lee NS, Srivastava S, Wong KA, French BT, Black BE, Foltz DR: **Inheritance of CENP-A Nucleosomes during DNA Replication Requires HJURP**. *Dev Cell* 2018, **47**:348-362.e347.
52. Hori T, Kagawa N, Toyoda A, Fujiyama A, Misu S, Monma N, Makino F, Ikeo K, Fukagawa T: **Constitutive centromere-associated network controls centromere drift in vertebrate cells**. *J Cell Biol* 2017, **216**:101-113.
53. Gonzalez M, He H, Dong Q, Sun S, Li F: **Ectopic centromere nucleation by CENP--a in fission yeast**. *Genetics* 2014, **198**:1433-1446.
54. Palladino J, Chavan A, Sposato A, Mason TD, Mellone BG: **Targeted De Novo Centromere Formation in Drosophila Reveals Plasticity and Maintenance Potential of CENP-A Chromatin**. *Dev Cell* 2020, **52**:379-394.e377.
55. Barnhart MC, Kuich PH, Stellfox ME, Ward JA, Bassett EA, Black BE, Foltz DR: **HJURP is a CENP-A chromatin assembly factor sufficient to form a functional de novo kinetochore**. *J Cell Biol* 2011, **194**:229-243.
56. Warburton PE: **Chromosomal dynamics of human neocentromere formation**. *Chromosome Res* 2004, **12**:617-626.
57. Scott KC, Sullivan BA: **Neocentromeres: a place for everything and everything in its place**. *Trends Genet* 2014, **30**:66-74.
58. Stimpson KM, Matheny JE, Sullivan BA: **Dicentric chromosomes: unique models to study centromere function and inactivation**. *Chromosome Res* 2012, **20**:595-605.
59. McIntosh JR, O'Toole E, Zhudenkov K, Morphew M, Schwartz C, Ataullakhanov FI, Grishchuk EL: **Conserved and divergent features of kinetochores and spindle microtubule ends from five species**. *J Cell Biol* 2013, **200**:459-474.
60. Zhang H, Dawe RK: **Total centromere size and genome size are strongly correlated in ten grass species**. *Chromosome Res* 2012, **20**:403-412.
61. McEwen BF, Chan GK, Zubrowski B, Savoian MS, Sauer MT, Yen TJ: **CENP-E is essential for reliable bioriented spindle attachment, but chromosome alignment can be achieved via redundant mechanisms in mammalian cells**. *Mol Biol Cell* 2001, **12**:2776-2789.
62. Burrack LS, Applen SE, Berman J: **The requirement for the Dam1 complex is dependent upon the number of kinetochore proteins and microtubules**. *Curr Biol* 2011, **21**:889-896.
63. Maiato H, DeLuca J, Salmon ED, Earnshaw WC: **The dynamic kinetochore-microtubule interface**. *J Cell Sci* 2004, **117**:5461-5477.
64. McEwen BF, Ding Y, Heagle AB: **Relevance of kinetochore size and microtubule-binding capacity for stable chromosome attachment during mitosis in PtK1 cells**. *Chromosome Res* 1998, **6**:123-132.
65. Moens PB: **Kinetochore microtubule numbers of different sized chromosomes**. *J Cell Biol* 1979, **83**:556-561.
66. Heath IB: **Variant mitoses in lower eukaryotes: indicators of the evolution of mitosis**. *Int Rev Cytol* 1980, **64**:1-80.
67. Kursel LE, Malik HS: **The cellular mechanisms and consequences of centromere drive**. *Curr Opin Cell Biol* 2018, **52**:58-65.
68. Henikoff S, Ahmad K, Malik HS: **The centromere paradox: stable inheritance with rapidly evolving DNA**. *Science* 2001, **293**:1098-1102.
69. Drinnenberg IA, Henikoff S, Malik HS: **Evolutionary Turnover of Kinetochore Proteins: A Ship of Theseus?** *Trends Cell Biol* 2016, **26**:498-510.
70. Burrack LS, Berman J: **Flexibility of centromere and kinetochore structures**. *Trends Genet* 2012, **28**:204-212.
71. Bloom KS, Carbon J: **Yeast centromere DNA is in a unique and highly ordered structure in chromosomes and small circular minichromosomes**. *Cell* 1982, **29**:305-317.
72. Furuyama S, Biggins S: **Centromere identity is specified by a single centromeric nucleosome in budding yeast**. *Proc Natl Acad Sci U S A* 2007, **104**:14706-14711.
73. Peter J, De Chiara M, Friedrich A, Yue JX, Pflieger D, Bergstrom A, Sigwalt A, Barre B, Freel K, Llored A, et al.: **Genome evolution across 1,011 Saccharomyces cerevisiae isolates**. *Nature* 2018, **556**:339-344.
74. Gasch AP, Hose J, Newton MA, Sardi M, Yong M, Wang Z: **Further support for aneuploidy tolerance in wild yeast and effects of dosage compensation on gene copy-number evolution**. *Elife* 2016, **5**:e14409.
75. Hamilton G, Dimitrova Y, Davis TN: **Seeing is believing: our evolving view of kinetochore structure, composition, and assembly**. *Curr Opin Cell Biol* 2019, **60**:44-52.
76. Tromer EC, van Hooff JJE, Kops G, Snel B: **Mosaic origin of the eukaryotic kinetochore**. *Proc Natl Acad Sci U S A* 2019, **116**:12873-12882.
77. De Wulf P, McAinsh AD, Sorger PK: **Hierarchical assembly of the budding yeast kinetochore from multiple subcomplexes**. *Genes Dev* 2003, **17**:2902-2921.
78. Jenni S, Harrison SC: **Structure of the DASH/Dam1 complex shows its role at the yeast kinetochore-microtubule interface**. *Science* 2018, **360**:552-558.
79. Legal T, Zou J, Sochaj A, Rappsilber J, Welburn JP: **Molecular architecture of the Dam1 complex-microtubule interaction**. *Open Biol* 2016, **6**.
80. Miranda JJ, De Wulf P, Sorger PK, Harrison SC: **The yeast DASH complex forms closed rings on microtubules**. *Nat Struct Mol Biol* 2005, **12**:138-143.
81. Welburn JP, Grishchuk EL, Backer CB, Wilson-Kubalek EM, Yates JR, Cheeseman IM: **The human kinetochore Ska1 complex facilitates microtubule depolymerization-coupled motility**. *Dev Cell* 2009, **16**:374-385.
82. Janczyk P, Skorupka KA, Tooley JG, Matson DR, Kestner CA, West T, Pornillos O, Stukenberg PT: **Mechanism of Ska Recruitment by Ndc80 Complexes to Kinetochores**. *Dev Cell* 2017, **41**:438-449.

83. Helgeson LA, Zelter A, Riffle M, MacCoss MJ, Asbury CL, Davis TN: **Human Ska complex and Ndc80 complex interact to form a load-bearing assembly that strengthens kinetochore-microtubule attachments**. *Proc Natl Acad Sci U S A* 2018, **115**:2740-2745.
84. Ciferri C, Pasqualato S, Screpanti E, Varetti G, Santaguida S, Dos Reis G, Maiolica A, Polka J, De Luca JG, De Wulf P, et al.: **Implications for kinetochore-microtubule attachment from the structure of an engineered Ndc80 complex**. *Cell* 2008, **133**:427-439.
85. Valverde R, Ingram J, Harrison SC: **Conserved Tetramer Junction in the Kinetochore Ndc80 Complex**. *Cell Rep* 2016, **17**:1915-1922.
86. Scarborough EA, Davis TN, Asbury CL: **Tight bending of the Ndc80 complex provides intrinsic regulation of its binding to microtubules**. *Elife* 2019, **8**.
87. Asbury CL, Gestaut DR, Powers AF, Franck AD, Davis TN: **The Dam1 kinetochore complex harnesses microtubule dynamics to produce force and movement**. *Proc Natl Acad Sci U S A* 2006, **103**:9873-9878.
88. Powers AF, Franck AD, Gestaut DR, Cooper J, Gracyzk B, Wei RR, Wordeman L, Davis TN, Asbury CL: **The Ndc80 kinetochore complex forms load-bearing attachments to dynamic microtubule tips via biased diffusion**. *Cell* 2009, **136**:865-875.
89. Umbreit NT, Miller MP, Tien JF, Ortola JC, Gui L, Lee KK, Biggins S, Asbury CL, Davis TN: **Kinetochores require oligomerization of Dam1 complex to maintain microtubule attachments against tension and promote biorientation**. *Nat Commun* 2014, **5**:4951.
90. Kim JO, Zelter A, Umbreit NT, Bollozos A, Riffle M, Johnson R, MacCoss MJ, Asbury CL, Davis TN: **The Ndc80 complex bridges two Dam1 complex rings**. *Elife* 2017, **6**.
91. Tien JF, Umbreit NT, Gestaut DR, Franck AD, Cooper J, Wordeman L, Gonen T, Asbury CL, Davis TN: **Cooperation of the Dam1 and Ndc80 kinetochore complexes enhances microtubule coupling and is regulated by aurora B**. *J Cell Biol* 2010, **189**:713-723.
92. Volkov VA, Huis In 't Veld PJ, Dogterom M, Musacchio A: **Multivalency of NDC80 in the outer kinetochore is essential to track shortening microtubules and generate forces**. *Elife* 2018, **7**.
93. Lampert F, Mieck C, Alushin GM, Nogales E, Westermann S: **Molecular requirements for the formation of a kinetochore-microtubule interface by Dam1 and Ndc80 complexes**. *J Cell Biol* 2013, **200**:21-30.
94. Cheeseman IM, Anderson S, Jwa M, Green EM, Kang J, Yates JR, Chan CS, Drubin DG, Barnes G: **Phospho-regulation of kinetochore-microtubule attachments by the Aurora kinase Ipl1p**. *Cell* 2002, **111**:163-172.
95. Cheeseman IM, Chappie JS, Wilson-Kubalek EM, Desai A: **The conserved KMN network constitutes the core microtubule-binding site of the kinetochore**. *Cell* 2006, **127**:983-997.
96. Caldas GV, DeLuca KF, DeLuca JG: **KNL1 facilitates phosphorylation of outer kinetochore proteins by promoting Aurora B kinase activity**. *J Cell Biol* 2013, **203**:957-969.
97. Sarangapani KK, Akiyoshi B, Duggan NM, Biggins S, Asbury CL: **Phosphoregulation promotes release of kinetochores from dynamic microtubules via multiple mechanisms**. *Proc Natl Acad Sci U S A* 2013, **110**:7282-7287.
98. Kudalkar EM, Scarborough EA, Umbreit NT, Zelter A, Gestaut DR, Riffle M, Johnson RS, MacCoss MJ, Asbury CL, Davis TN: **Regulation of outer kinetochore Ndc80 complex-based microtubule attachments by the central kinetochore Mis12/MIND complex**. *Proc Natl Acad Sci U S A* 2015, **112**:E5583-5589.
99. Dimitrova YN, Jenni S, Valverde R, Khin Y, Harrison SC: **Structure of the MIND Complex Defines a Regulatory Focus for Yeast Kinetochore Assembly**. *Cell* 2016, **167**:1014-1027.
100. Joglekar AP, Bouck DC, Molk JN, Bloom KS, Salmon ED: **Molecular architecture of a kinetochore-microtubule attachment site**. *Nat Cell Biol* 2006, **8**:581-585.
101. Schmitzberger F, Richter MM, Gordiyenko Y, Robinson CV, Dadlez M, Westermann S: **Molecular basis for inner kinetochore configuration through RWD domain-peptide interactions**. *Embo j* 2017, **36**:3458-3482.
102. Biggins S: **The composition, functions, and regulation of the budding yeast kinetochore**. *Genetics* 2013, **194**:817-846.
103. Hinshaw SM, Harrison SC: **The structure of the Ctf19c/CCAN from budding yeast**. *Elife* 2019, **8**.
104. Lang J, Barber A, Biggins S: **An assay for de novo kinetochore assembly reveals a key role for the CENP-T pathway in budding yeast**. *Elife* 2018, **7**.
105. Pekgöz Altunkaya G, Malvezzi F, Demianova Z, Zimniak T, Litos G, Weissmann F, Mechtler K, Herzog F, Westermann S: **CCAN Assembly Configures Composite Binding Interfaces to Promote Cross-Linking of Ndc80 Complexes at the Kinetochore**. *Curr Biol* 2016, **26**:2370-2378.
106. Hyland KM, Kingsbury J, Koshland D, Hieter P: **Ctf19p: A novel kinetochore protein in Saccharomyces cerevisiae and a potential link between the kinetochore and mitotic spindle**. *J Cell Biol* 1999, **145**:15-28.
107. Hornung P, Troc P, Malvezzi F, Maier M, Demianova Z, Zimniak T, Litos G, Lampert F, Schleiffer A, Brunner M, et al.: **A cooperative mechanism drives budding yeast kinetochore assembly downstream of CENP-A**. *J Cell Biol* 2014, **206**:509-524.
108. Petrovic A, Keller J, Liu Y, Overlack K, John J, Dimitrova YN, Jenni S, van Gerwen S, Stege P, Wohlgemuth S, et al.: **Structure of the MIS12 Complex and Molecular Basis of Its Interaction with CENP-C at Human Kinetochores**. *Cell* 2016, **167**:1028-1040.
109. Fischbock-Halwachs J, Singh S, Potocnjak M, Hagemann G, Solis-Mezarino V, Woike S, Ghodgaonkar-Steger M, Weissmann F, Gallego LD, Rojas J, et al.: **The COMA complex interacts with Cse4 and positions Sli15/Ipl1 at the budding yeast inner kinetochore**. *Elife* 2019, **8**.
110. Anedchenko EA, Samel-Pommerencke A, Tran Nguyen TM, Shahnejat-Bushehri S, Pöpsel J, Lauster D, Herrmann A, Rappsilber J, Cuomo A, Bonaldi T, et al.: **The kinetochore module Okp1 CENP-Q /Ame1 CENP-U is a reader for N-terminal modifications on the centromeric histone Cse4 CENP-A**. *EMBO Journal* 2019, **38**.
111. Pesenti ME, Prumbaum D, Auckland P, Smith CM, Faesen AC, Petrovic A, Erent M, Maffini S, Pentakota S, Weir JR, et al.: **Reconstitution of a 26-Subunit Human Kinetochore Reveals Cooperative Microtubule Binding by CENP-OPQUR and NDC80**. *Mol Cell* 2018, **71**:923-939.
112. Meeks-Wagner D, Wood JS, Garvik B, Hartwell LH: **Isolation of two genes that affect mitotic chromosome transmission in S. cerevisiae**. *Cell* 1986, **44**:53-63.
113. Brown MT, Goetsch L, Hartwell LH: **MIF2 is required for mitotic spindle integrity during anaphase spindle elongation in Saccharomyces cerevisiae**. *J Cell Biol* 1993, **123**:387-403.
114. Cohen RL, Espelin CW, De Wulf P, Sorger PK, Harrison SC, Simons KT: **Structural and functional dissection of Mif2p, a conserved DNA-binding kinetochore protein**. *Mol Biol Cell* 2008, **19**:4480-4491.
115. Chik JK, Moiseeva V, Goel PK, Meinen BA, Koldewey P, An S, Mellone BG, Subramanian L, Cho US: **Structures of CENP-C cupin domains at regional centromeres reveal unique patterns of dimerization and recruitment functions for the inner pocket**. *J Biol Chem* 2019, **294**:14119-14134.

116. Kato H, Jiang J, Zhou BR, Rozendaal M, Feng H, Ghirlando R, Xiao TS, Straight AF, Bai Y: **A conserved mechanism for centromeric nucleosome recognition by centromere protein CENP-C**. *Science* 2013, **340**:1110-1113.
117. Ortiz J, Stemmann O, Rank S, Lechner J: **A putative protein complex consisting of Ctf19, Mcm21, and Okp1 represents a missing link in the budding yeast kinetochore**. *Genes Dev* 1999, **13**:1140-1155.
118. Xiao H, Wang F, Wisniewski J, Shaytan AK, Ghirlando R, FitzGerald PC, Huang Y, Wei D, Li S, Landsman D, et al.: **Molecular basis of CENP-C association with the CENP-A nucleosome at yeast centromeres**. *Genes Dev* 2017, **31**:1958-1972.
119. Carroll CW, Milks KJ, Straight AF: **Dual recognition of CENP-A nucleosomes is required for centromere assembly**. *J Cell Biol* 2010, **189**:1143-1155.
120. Guse A, Carroll CW, Moree B, Fuller CJ, Straight AF: **In vitro centromere and kinetochore assembly on defined chromatin templates**. *Nature* 2011, **477**:354-358.
121. Krizaic I, Williams SJ, Sánchez P, Rodríguez-Corsino M, Stukenberg PT, Losada A: **The distinct functions of CENP-C and CENP-T/W in centromere propagation and function in Xenopus egg extracts**. *Nucleus* 2015, **6**:133-143.
122. Liu Y, Petrovic A, Rombaut P, Mosalaganti S, Keller J, Raunser S, Herzog F, Musacchio A: **Insights from the reconstitution of the divergent outer kinetochore of Drosophila melanogaster**. *Open Biol* 2016, **6**:150236.
123. van Hooff JJ, Tromer E, van Wijk LM, Snel B, Kops GJ: **Evolutionary dynamics of the kinetochore network in eukaryotes as revealed by comparative genomics**. *EMBO Rep* 2017, **18**:1559-1571.
124. Yan K, Yang J, Zhang Z, McLaughlin SH, Chang L, Fasci D, Ehrenhofer-Murray AE, Heck AJR, Barford D: **Structure of the inner kinetochore CCAN complex assembled onto a centromeric nucleosome**. *Nature* 2019, **574**:278-282.
125. Sullivan KF, Hechenberger M, Masri K: **Human CENP-A contains a histone H3 related histone fold domain that is required for targeting to the centromere**. *J Cell Biol* 1994, **127**:581-592.
126. Earnshaw WC, Migeon BR: **Three related centromere proteins are absent from the inactive centromere of a stable isodicentric chromosome**. *Chromosoma* 1985, **92**:290-296.
127. Akiyoshi B: **The unconventional kinetoplastid kinetochore: from discovery toward functional understanding**. *Biochem Soc Trans* 2016, **44**:1201-1217.
128. Drinnenberg IA, deYoung D, Henikoff S, Malik HS: **Recurrent loss of CenH3 is associated with independent transitions to holocentricity in insects**. *Elife* 2014, **3**.
129. Lawrimore J, Bloom KS, Salmon ED: **Point centromeres contain more than a single centromere-specific Cse4 (CENP-A) nucleosome**. *J Cell Biol* 2011, **195**:573-582.
130. Aravamudhan P, Felzer-Kim I, Joglekar AP: **The budding yeast point centromere associates with two Cse4 molecules during mitosis**. *Curr Biol* 2013, **23**:770-774.
131. Coffman VC, Wu P, Parthun MR, Wu JQ: **CENP-A exceeds microtubule attachment sites in centromere clusters of both budding and fission yeast**. *J Cell Biol* 2011, **195**:563-572.
132. Henikoff S, Henikoff JG: **"Point" centromeres of Saccharomyces harbor single centromere-specific nucleosomes**. *Genetics* 2012, **190**:1575-1577.
133. Henikoff S, Ramachandran S, Krassovsky K, Bryson TD, Codomo CA, Brogaard K, Widom J, Wang J-P, Henikoff JG, Struhl K: **The budding yeast Centromere DNA Element II wraps a stable Cse4 hemisome in either orientation in vivo**. *eLife* 2014, **3**.
134. Camahort R, Shivaraju M, Mattingly M, Li B, Nakanishi S, Zhu D, Shilatifard A, Workman JL, Gerton JL: **Cse4 Is Part of an Octameric Nucleosome in Budding Yeast**. *Molecular Cell* 2009, **35**:794-805.
135. Sekulic N, Bassett EA, Rogers DJ, Black BE: **The structure of (CENP-A-H4)(2) reveals physical features that mark centromeres**. *Nature* 2010, **467**:347-351.
136. Tachiwana H, Kagawa W, Shiga T, Osakabe A, Miya Y, Saito K, Hayashi-Takanaka Y, Oda T, Sato M, Park S-Y, et al.: **Crystal structure of the human centromeric nucleosome containing CENP-A**. *Nature* 2011, **476**:232.
137. Williams JS, Hayashi T, Yanagida M, Russell P: **Fission yeast Scm3 mediates stable assembly of Cnp1/CENP-A into centromeric chromatin**. *Mol Cell* 2009, **33**:287-298.
138. Mizuguchi G, Xiao H, Wisniewski J, Smith MM, Wu C: **Nonhistone Scm3 and histones CenH3-H4 assemble the core of centromere-specific nucleosomes**. *Cell* 2007, **129**:1153-1164.
139. Furuyama T, Henikoff S: **Centromeric nucleosomes induce positive DNA supercoils**. *Cell* 2009, **138**:104-113.
140. Black BE, Cleveland DW: **Epigenetic centromere propagation and the nature of CENP-a nucleosomes**. *Cell* 2011, **144**:471-479.
141. Bui M, Dimitriadis Emilios k, Hoischen C, An E, Quénet D, Giebe S, Nita-Lazar A, Diekmann S, Dalal Y: **Cell-Cycle-Dependent Structural Transitions in the Human CENP-A Nucleosome In Vivo**. *Cell* 2012, **150**:317-326.
142. Shivaraju M, Unruh JR, Slaughter BD, Mattingly M, Berman J, Gerton JL: **Cell-cycle-coupled structural oscillation of centromeric nucleosomes in yeast**. *Cell* 2012, **150**:304-316.
143. Nechemia-Arbely Y, Fachinetti D, Miga KH, Sekulic N, Soni GV, Kim DH, Wong AK, Lee AY, Nguyen K, Dekker C, et al.: **Human centromeric CENP-A chromatin is a homotypic, octameric nucleosome at all cell cycle points**. *The Journal of Cell Biology* 2017, **216**:607-621.
144. Mishra PK, Basrai MA: **Protein kinases in mitotic phosphorylation of budding yeast CENP-A**. *Curr Genet* 2019, **65**:1325-1332.
145. Boeckmann L, Takahashi Y, Au WC, Mishra PK, Choy JS, Dawson AR, Szeto MY, Waybright TJ, Heger C, McAndrew C, et al.: **Phosphorylation of centromeric histone H3 variant regulates chromosome segregation in Saccharomyces cerevisiae**. *Mol Biol Cell* 2013, **24**:2034-2044.
146. Nicklas RB: **The forces that move chromosomes in mitosis**. *Annu Rev Biophys Biophys Chem* 1988, **17**:431-449.
147. Joglekar AP, Bloom K, Salmon ED: **In vivo protein architecture of the eukaryotic kinetochore with nanometer scale accuracy**. *Curr Biol* 2009, **19**:694-699.
148. Brock JA, Bloom K: **A chromosome breakage assay to monitor mitotic forces in budding yeast**. *J Cell Sci* 1994, **107 (Pt 4)**:891-902.
149. Fisher JK, Ballenger M, O'Brien ET, Haase J, Superfine R, Bloom K: **DNA relaxation dynamics as a probe for the intracellular environment**. *Proc Natl Acad Sci U S A* 2009, **106**:9250-9255.
150. Chacon JM, Mukherjee S, Schuster BM, Clarke DJ, Gardner MK: **Pericentromere tension is self-regulated by spindle structure in metaphase**. *J Cell Biol* 2014, **205**:313-324.
151. Alexander SP, Rieder CL: **Chromosome motion during attachment to the vertebrate spindle: initial saltatory-like behavior of chromosomes and quantitative analysis of force production by nascent kinetochore fibers**. *J Cell Biol* 1991, **113**:805-815.

152. Ye AA, Cane S, Maresca TJ: **Chromosome biorientation produces hundreds of piconewtons at a metazoan kinetochore**. *Nat Commun* 2016, **7**:13221.
153. Suzuki A, Badger BL, Haase J, Ohashi T, Erickson HP, Salmon ED, Bloom K: **How the kinetochore couples microtubule force and centromere stretch to move chromosomes**. *Nat Cell Biol* 2016, **18**:382-392.
154. Rieder CL, Schultz A, Cole R, Sluder G: **Anaphase onset in vertebrate somatic cells is controlled by a checkpoint that monitors sister kinetochore attachment to the spindle**. *J Cell Biol* 1994, **127**:1301-1310.
155. Rieder CL, Salmon ED: **The vertebrate cell kinetochore and its roles during mitosis**. *Trends Cell Biol* 1998, **8**:310-318.
156. Cimini D, Howell B, Maddox P, Khodjakov A, Degrassi F, Salmon ED: **Merotelic kinetochore orientation is a major mechanism of aneuploidy in mitotic mammalian tissue cells**. *J Cell Biol* 2001, **153**:517-527.
157. Cimini D, Fioravanti D, Salmon ED, Degrassi F: **Merotelic kinetochore orientation versus chromosome mono-orientation in the origin of lagging chromosomes in human primary cells**. *J Cell Sci* 2002, **115**:507-515.
158. Khodjakov A, Pines J: **Centromere tension: a divisive issue**. *Nat Cell Biol* 2010, **12**:919-923.
159. Nicklas RB, Koch CA: **Chromosome micromanipulation. 3. Spindle fiber tension and the reorientation of mal-oriented chromosomes**. *J Cell Biol* 1969, **43**:40-50.
160. Meraldi P, Draviam VM, Sorger PK: **Timing and checkpoints in the regulation of mitotic progression**. *Dev Cell* 2004, **7**:45-60.
161. Umbreit NT, Davis TN: **Mitosis puts sisters in a strained relationship: force generation at the kinetochore**. *Exp Cell Res* 2012, **318**:1361-1366.
162. Biggins S, Murray AW: **The budding yeast protein kinase Ipl1/Aurora allows the absence of tension to activate the spindle checkpoint**. *Genes Dev* 2001, **15**:3118-3129.
163. Pinsky BA, Kung C, Shokat KM, Biggins S: **The Ipl1-Aurora protein kinase activates the spindle checkpoint by creating unattached kinetochores**. *Nat Cell Biol* 2006, **8**:78-83.
164. Rieder CL, Cole RW, Khodjakov A, Sluder G: **The checkpoint delaying anaphase in response to chromosome monoorientation is mediated by an inhibitory signal produced by unattached kinetochores**. *J Cell Biol* 1995, **130**:941-948.
165. Hoyt MA, Totis L, Roberts BT: **S. cerevisiae genes required for cell cycle arrest in response to loss of microtubule function**. *Cell* 1991, **66**:507-517.
166. Collin P, Nashchekina O, Walker R, Pines J: **The spindle assembly checkpoint works like a rheostat rather than a toggle switch**. *Nat Cell Biol* 2013, **15**:1378-1385.
167. Ciliberto A, Hauf S: **Micromanaging checkpoint proteins**. *Elife* 2017, **6**.
168. Faesen AC, Thanasoula M, Maffini S, Breit C, Müller F, van Gerwen S, Bange T, Musacchio A: **Basis of catalytic assembly of the mitotic checkpoint complex**. *Nature* 2017, **542**:498-502.
169. De Antoni A, Pearson CG, Cimini D, Canman JC, Sala V, Nezi L, Mapelli M, Sironi L, Faretta M, Salmon ED, et al.: **The Mad1/Mad2 complex as a template for Mad2 activation in the spindle assembly checkpoint**. *Curr Biol* 2005, **15**:214-225.
170. Musacchio A, Salmon ED: **The spindle-assembly checkpoint in space and time**. *Nat Rev Mol Cell Biol* 2007, **8**:379-393.
171. Meadows JC, Shepperd LA, Vanoosthuyse V, Lancaster TC, Sochaj AM, Buttrick GJ, Hardwick KG, Millar JB: **Spindle checkpoint silencing requires association of PP1 to both Spc7 and kinesin-8 motors**. *Dev Cell* 2011, **20**:739-750.
172. London N, Ceto S, Ranish JA, Biggins S: **Phosphoregulation of Spc105 by Mps1 and PP1 regulates Bub1 localization to kinetochores**. *Curr Biol* 2012, **22**:900-906.
173. Rosenberg JS, Cross FR, Funabiki H: **KNL1/Spc105 recruits PP1 to silence the spindle assembly checkpoint**. *Curr Biol* 2011, **21**:942-947.
174. Lesage B, Qian J, Bollen M: **Spindle checkpoint silencing: PP1 tips the balance**. *Curr Biol* 2011, **21**:R898-903.
175. Santaguida S, Vernieri C, Villa F, Ciliberto A, Musacchio A: **Evidence that Aurora B is implicated in spindle checkpoint signalling independently of error correction**. *EMBO J* 2011, **30**:1508-1519.
176. Maresca TJ, Salmon ED: **Welcome to a new kind of tension: translating kinetochore mechanics into a wait-anaphase signal**. *J Cell Sci* 2010, **123**:825-835.
177. Byrne T, Coleman HG, Cooper JA, McCluggage WG, McCann A, Furlong F: **The association between MAD2 and prognosis in cancer: a systematic review and meta-analyses**. *Oncotarget* 2017, **8**:102223-102234.
178. Kops GJ, Weaver BA, Cleveland DW: **On the road to cancer: aneuploidy and the mitotic checkpoint**. *Nat Rev Cancer* 2005, **5**:773-785.
179. Lu S, Qian J, Guo M, Gu C, Yang Y: **Insights into a Crucial Role of TRIP13 in Human Cancer**. *Comput Struct Biotechnol J* 2019, **17**:854-861.
180. Ashkin A: **Acceleration and Trapping of Particles by Radiation Pressure**. *Physical Review Letters* 1970, **24**.
181. Killian JL, Ye F, Wang MD: **Optical Tweezers: A Force to Be Reckoned With**. *Cell* 2018, **175**:1445-1448.
182. Finer JT, Simmons RM, Spudich JA: **Single myosin molecule mechanics: piconewton forces and nanometre steps**. *Nature* 1994, **368**:113-119.
183. Kaseda K, Higuchi H, Hirose K: **Alternate fast and slow stepping of a heterodimeric kinesin molecule**. *Nat Cell Biol* 2003, **5**:1079-1082.
184. Asbury CL, Fehr AN, Block SM: **Kinesin moves by an asymmetric hand-over-hand mechanism**. *Science* 2003, **302**:2130-2134.
185. Merz AJ, So M, Sheetz MP: **Pilus retraction powers bacterial twitching motility**. *Nature* 2000, **407**:98-102.
186. Wang MD, Schnitzer MJ, Yin H, Landick R, Gelles J, Block SM: **Force and velocity measured for single molecules of RNA polymerase**. *Science* 1998, **282**:902-907.
187. Smith SB, Cui Y, Bustamante C: **Overstretching B-DNA: the elastic response of individual double-stranded and single-stranded DNA molecules**. *Science* 1996, **271**:795-799.
188. Smith SB, Finzi L, Bustamante C: **Direct mechanical measurements of the elasticity of single DNA molecules by using magnetic beads**. *Science* 1992, **258**:1122-1126.
189. Akiyoshi B, Sarangapani KK, Powers AF, Nelson CR, Reichow SL, Arellano-Santoyo H, Gonen T, Ranish JA, Asbury CL, Biggins S: **Tension directly stabilizes reconstituted kinetochore- microtubule attachments**. *Nature* 2010, **468**:576.
190. de Regt A, Asbury C, Biggins S: **Tension on kinetochore substrates is insufficient to prevent Aurora-triggered detachment**. Edited by. BioRxiv [Preprint]; 2018.
191. Gestaut DR, Graczyk B, Cooper J, Widlund PO, Zelter A, Wordeman L, Charles LA, Trisha ND: **Phosphoregulation and depolymerization- driven movement of the Dam1 complex do not require ring formation**. *Nature Cell Biology* 2008, **10**:407.
192. Franck AD, Powers AF, Gestaut DR, Gonen T, Davis TN, Asbury CL: **Tension applied through the Dam1 complex promotes microtubule elongation providing a direct mechanism for length control in mitosis**. *Nat Cell Biol* 2007, **9**:832-837.

193. Lampert F, Hornung P, Westermann S: **The Dam1 complex confers microtubule plus end-tracking activity to the Ndc80 kinetochore complex**. *J Cell Biol* 2010, **189**:641-649.
194. Weir JR, Faesen AC, Klare K, Petrovic A, Basilico F, Fischböck J, Pentakota S, Keller J, Pesenti ME, Pan D, et al.: **Insights from biochemical reconstitution into the architecture of human kinetochores**. *Nature* 2016, **537**:249-253.
195. Cimini D: **Merotelic kinetochore orientation, aneuploidy, and cancer**. *Biochim Biophys Acta* 2008, **1786**:32-40.
196. Musacchio A, Desai A: **A Molecular View of Kinetochore Assembly and Function**. *Biology (Basel)* 2017, **6**.
197. Musacchio A: **Spindle assembly checkpoint: the third decade**. *Philos Trans R Soc Lond B Biol Sci* 2011, **366**:3595-3604.
198. Nicklas RB, Ward SC: **Elements of error correction in mitosis: microtubule capture, release, and tension**. *J Cell Biol* 1994, **126**:1241-1253.
199. Westermann S, Schleiffer A: **Family matters: structural and functional conservation of centromere-associated proteins from yeast to humans**. *Trends Cell Biol* 2013, **23**:260-269.
200. Miller MP, Asbury CL, Biggins S: **A TOG Protein Confers Tension Sensitivity to Kinetochore-Microtubule Attachments**. *Cell* 2016, **165**:1428-1439.
201. Pot I, Knockleby J, Aneliunas V, Nguyen T, Ah-Kye S, Liszt G, Snyder M, Hieter P, Vogel J: **Spindle checkpoint maintenance requires Ame1 and Okp1**. *Cell Cycle* 2005, **4**:1448-1456.
202. Hara M, Fukagawa T: **Critical Foundation of the Kinetochore: The Constitutive Centromere-Associated Network (CCAN)**. *Prog Mol Subcell Biol* 2017, **56**:29-57.
203. Screpanti E, De Antoni A, Alushin GM, Petrovic A, Melis T, Nogales E, Musacchio A: **Direct binding of Cenp-C to the Mis12 complex joins the inner and outer kinetochore**. *Curr Biol* 2011, **21**:391-398.
204. Wei RR, Sorger PK, Harrison SC: **Molecular organization of the Ndc80 complex, an essential kinetochore component**. *Proc Natl Acad Sci U S A* 2005, **102**:5363-5367.
205. Migl D, Kschonsak M, Arthur CP, Khin Y, Harrison SC, Ciferri C, Dimitrova YN: **Cryoelectron Microscopy Structure of a Yeast Centromeric Nucleosome at 2.7 Å Resolution**. *Structure* 2020, **28**:1-8.
206. Franck AD, Powers AF, Gestaut DR, Davis TN, Asbury CL: **Direct physical study of kinetochore-microtubule interactions by reconstitution and interrogation with an optical force clamp**. *Methods* 2010, **51**:242-250.
207. Hinshaw SM, Harrison SC: **An Iml3-Chl4 heterodimer links the core centromere to factors required for accurate chromosome segregation**. *Cell Rep* 2013, **5**:29-36.
208. Lowary PT, Widom J: **New DNA sequence rules for high affinity binding to histone octamer and sequence-directed nucleosome positioning**. *J Mol Biol* 1998, **276**:19-42.
209. Team RC: **R: A Language and Environment for Statistical Computing**. Edited by. Vienna, Austria; 2013.
210. Wickham H: **ggplot2: Elegant Graphics for Data Analysis**. Edited by: Springer-Verlag New York; 2009.
211. Kassambra A, Kosiniski M: **survminer: Drawing Survival Curves using 'ggplot2'**. Edited by; 2018.
212. Fischboeck J, Singh S, Potocnjak M, Hagemann G, Solis V, Woike S, Ghodgaonkar M, Andreani J, Herzog F: **The COMA complex is required for positioning Ipl1 activity proximal to Cse4 nucleosomes in budding yeast**. *bioRxiv* 2018:444570.
213. Palmer DK, O'Day K, Trong HL, Charbonneau H, Margolis RL: **Purification of the centromere-specific protein CENP-A and demonstration that it is a distinctive histone**. *Proc Natl Acad Sci U S A* 1991, **88**:3734-3738.
214. Stoler S, Keith KC, Curnick KE, Fitzgerald-Hayes M: **A mutation in CSE4, an essential gene encoding a novel chromatin-associated protein in yeast, causes chromosome nondisjunction and cell cycle arrest at mitosis**. *Genes Dev* 1995, **9**:573-586.
215. Dhatchinamoorthy K, Shivaraju M, Lange JJ, Rubinstein B, Unruh JR, Slaughter BD, Gerton JL: **Structural plasticity of the living kinetochore**. *The Journal of cell biology* 2017, **216**:3551.
216. Kagawa N, Hori T, Hoki Y, Hosoya O, Tsutsui K, Saga Y, Sado T, Fukagawa T: **The CENP-O complex requirement varies among different cell types**. *Chromosome Res* 2014, **22**:293-303.
217. Bock LJ, Pagliuca C, Kobayashi N, Grove RA, Oku Y, Shrestha K, Alfieri C, Golfieri C, Oldani A, Dal Maschio M, et al.: **Cnn1 inhibits the interactions between the KMN complexes of the yeast kinetochore**. *Nat Cell Biol* 2012, **14**:614-624.
218. Huis In 't Veld PJ, Jeganathan S, Petrovic A, Singh P, John J, Krenn V, Weissmann F, Bange T, Musacchio A: **Molecular basis of outer kinetochore assembly on CENP-T**. *Elife* 2016, **5**.
219. Giaever G, Chu AM, Ni L, Connelly C, Riles L, Veronneau S, Dow S, Lucau-Danila A, Anderson K, Andre B, et al.: **Functional profiling of the Saccharomyces cerevisiae genome**. *Nature* 2002, **418**:387-391.
220. Gascoigne KE, Takeuchi K, Suzuki A, Hori T, Fukagawa T, Cheeseman IM: **Induced ectopic kinetochore assembly bypasses the requirement for CENP-A nucleosomes**. *Cell* 2011, **145**:410-422.
221. Nishino T, Rago F, Hori T, Tomii K, Cheeseman IM, Fukagawa T: **CENP-T provides a structural platform for outer kinetochore assembly**. *Embo j* 2013, **32**:424-436.
222. Schleiffer A, Maier M, Litos G, Lampert F, Hornung P, Mechtler K, Westermann S: **CENP-T proteins are conserved centromere receptors of the Ndc80 complex**. *Nat Cell Biol* 2012, **14**:604-613.
223. Zelter A, Bonomi M, Kim J, Umbreit N, Hoopmann M, Johnson R, Riffle M, Jaschob D, Maccoss M, Moritz R, et al.: **The molecular architecture of the Dam1 kinetochore complex is defined by cross-linking based structural modelling**. *Nature Communications* 2015, **6**:8673.
224. Chambers MC, Maclean B, Burke R, Amodei D, Ruderman DL, Neumann S, Gatto L, Fischer B, Pratt B, Egertson J, et al.: **A cross-platform toolkit for mass spectrometry and proteomics**. In *Nat Biotechnol*. Edited by; 2012:918-920. vol 30.]
225. Hoopmann MR, Zelter A, Johnson RS, Riffle M, MacCoss MJ, Davis TN, Moritz RL: **Kojak: efficient analysis of chemically cross-linked protein complexes**. *J Proteome Res* 2015, **14**:2190-2198.
226. Kall L, Canterbury JD, Weston J, Noble WS, MacCoss MJ: **Semi-supervised learning for peptide identification from shotgun proteomics datasets**. *Nat Methods* 2007, **4**:923-925.
227. Riffle M, Jaschob D, Zelter A, Davis TN: **ProXL (Protein Cross-Linking Database): A Platform for Analysis, Visualization, and Sharing of Protein Cross-Linking Mass Spectrometry Data**. *J Proteome Res* 2016, **15**:2863-2870.
228. Riffle M, Jaschob D, Zelter A, Davis TN: **Proxl (Protein Cross-Linking Database): A Public Server, QC Tools, and Other Major Updates**. *J Proteome Res* 2019, **18**:759-764.
229. Deyaert E, Wauters L, Guaitoli G, Konijnenberg A, Leemans M, Terheyden S, Petrovic A, Gallardo R, Nederveen-Schippers LM, Athanasopoulos PS, et al.: **A homologue of the Parkinson's disease-associated protein LRRK2 undergoes a monomer-dimer transition during GTP turnover**. *Nat Commun* 2017, **8**:1008.

230. Thawani A, Stone HA, Shaevitz JW, Petry S: **Molecular mechanism of microtubule nucleation from gamma-tubulin ring complex**. Edited by: bioRxiv; 2019.
231. Wieczorek M, Bechstedt S, Chaaban S, Brouhard GJ: **Microtubule-associated proteins control the kinetics of microtubule nucleation**. *Nat Cell Biol* 2015, **17**:907-916.
232. Hagan MF: **Modeling Viral Capsid Assembly**. *Adv Chem Phys* 2014, **155**:1-68.
233. Inoue S, Sugiyama S, Travers AA, Ohyama T: **Self-assembly of double-stranded DNA molecules at nanomolar concentrations**. *Biochemistry* 2007, **46**:164-171.
234. Deyter GM, Hildebrand EM, Barber AD, Biggins S: **Histone H4 Facilitates the Proteolysis of the Budding Yeast CENP-ACse4 Centromeric Histone Variant**. *Genetics* 2017, **205**:113-124.
235. Chittori S, Hong J, Saunders H, Feng H, Ghirlando R, Kelly AE, Bai Y, Subramaniam S: **Structural mechanisms of centromeric nucleosome recognition by the kinetochore protein CENP-N**. *Science (New York, N.Y.)* 2017, **359**.
236. DeLuca KF, Lens SM, DeLuca JG: **Temporal changes in Hec1 phosphorylation control kinetochore-microtubule attachment stability during mitosis**. *J Cell Sci* 2011, **124**:622-634.
237. DeLuca KF, Meppelink A, Broad AJ, Mick JE, Peersen OB, Pektas S, Lens SMA, DeLuca JG: **Aurora A kinase phosphorylates Hec1 to regulate metaphase kinetochore-microtubule dynamics**. *J Cell Biol* 2018, **217**:163-177.
238. Shang C, Hazbun TR, Cheeseman IM, Aranda J, Fields S, Drubin DG, Barnes G: **Kinetochore protein interactions and their regulation by the Aurora kinase Ipl1p**. *Mol Biol Cell* 2003, **14**:3342-3355.
239. Krenn V, Musacchio A: **The Aurora B Kinase in Chromosome Bi-Orientation and Spindle Checkpoint Signaling**. *Front Oncol* 2015, **5**:225.
240. Cho US, Harrison SC: **Ndc10 is a platform for inner kinetochore assembly in budding yeast**. *Nat Struct Mol Biol* 2011, **19**:48-55.
241. Funabiki H: **Correcting aberrant kinetochore microtubule attachments: a hidden regulation of Aurora B on microtubules**. *Curr Opin Cell Biol* 2019, **58**:34-41.
242. Cormier A, Drubin DG, Barnes G: **Phosphorylation regulates kinase and microtubule binding activities of the budding yeast chromosomal passenger complex in vitro**. *J Biol Chem* 2013, **288**:23203-23211.
243. Tseng BS, Tan L, Kapoor TM, Funabiki H: **Dual detection of chromosomes and microtubules by the chromosomal passenger complex drives spindle assembly**. *Dev Cell* 2010, **18**:903-912.
244. García-Rodríguez LJ, Kasciukovic T, Denninger V, Tanaka TU: **Aurora B-INCENP Localization at Centromeres/Inner Kinetochores Is Required for Chromosome Bi-orientation in Budding Yeast**. *Curr Biol* 2019, **29**:1536-1544.e1534.
245. Liu D, Vader G, Vromans MJ, Lampson MA, Lens SM: **Sensing chromosome bi-orientation by spatial separation of aurora B kinase from kinetochore substrates**. *Science* 2009, **323**:1350-1353.
246. Wang E, Ballister ER, Lampson MA: **Aurora B dynamics at centromeres create a diffusion-based phosphorylation gradient**. *J Cell Biol* 2011, **194**:539-549.
247. Campbell CS, Desai A: **Tension sensing by Aurora B kinase is independent of survivin-based centromere localization**. *Nature* 2013, **497**:118-121.
248. Fink S, Turnbull K, Desai A, Campbell CS: **An engineered minimal chromosomal passenger complex reveals a role for INCENP/Sli15 spindle association in chromosome biorientation**. *J Cell Biol* 2017, **216**:911-923.
249. Hengeveld RCC, Vromans MJM, Vleugel M, Hadders MA, Lens SMA: **Inner centromere localization of the CPC maintains centromere cohesion and allows mitotic checkpoint silencing**. *Nat Commun* 2017, **8**:15542.
250. Yue Z, Carvalho A, Xu Z, Yuan X, Cardinale S, Ribeiro S, Lai F, Ogawa H, Gudmundsdottir E, Gassmann R, et al.: **Deconstructing Survivin: comprehensive genetic analysis of Survivin function by conditional knockout in a vertebrate cell line**. *J Cell Biol* 2008, **183**:279-296.
251. Tanaka TU, Rachidi N, Janke C, Pereira G, Galova M, Schiebel E, Stark MJ, Nasmyth K: **Evidence that the Ipl1-Sli15 (Aurora kinase-INCENP) complex promotes chromosome bi-orientation by altering kinetochore-spindle pole connections**. *Cell* 2002, **108**:317-329.
252. Bonner MK, Haase J, Swinderman J, Halas H, Miller Jenkins LM, Kelly AE: **Enrichment of Aurora B kinase at the inner kinetochore controls outer kinetochore assembly**. *J Cell Biol* 2019, **218**:3237-3257.
253. Costanzo M, VanderSluis B, Koch EN, Baryshnikova A, Pons C, Tan G, Wang W, Usaj M, Hanchard J, Lee SD, et al.: **A global genetic interaction network maps a wiring diagram of cellular function**. *Science* 2016, **353**.
254. Kuzmin E, VanderSluis B, Wang W, Tan G, Deshpande R, Chen Y, Usaj M, Balint A, Mattiazzi Usaj M, van Leeuwen J, et al.: **Systematic analysis of complex genetic interactions**. *Science* 2018, **360**.
255. Measday V, Baetz K, Guzzo J, Yuen K, Kwok T, Sheikh B, Ding H, Ueta R, Hoac T, Cheng B, et al.: **Systematic yeast synthetic lethal and synthetic dosage lethal screens identify genes required for chromosome segregation**. *Proc Natl Acad Sci U S A* 2005, **102**:13956-13961.

GRACE ELIZABETH HAMILTON

Vita

EDUCATION

- Bachelor of Science (2015) in Biology and Russian, Bates College, Lewiston, Maine.
- Doctor of Philosophy (2020) in Biochemistry, University of Washington, Seattle, Washington.

RESEARCH EXPERIENCE

- Doctoral thesis work with Dr. Trisha N. Davis (2015-2020), University of Washington, Seattle, Washington.
- Undergraduate thesis work with Dr. Rachel N. Austin (2014-2015), Bates College, Lewiston, Maine.
- Undergraduate research assistant (2013-2015), Bates College, Lewiston, Maine.

TEACHING EXPERIENCE

- Teaching assistant (2016-2017), University of Washington, Department of Biochemistry
- CLUE tutor (Winter 2018, Autumn 2019), University of Washington, Department of Biochemistry.
- Peer Writing Assistant (2012-2015), Bates College

PUBLICATIONS

- **Hamilton, G.E**., Helgeson, L.A., Noland, C., Asbury, C.L., Dimitrova, Y.N., and Davis, T.N. Reconstitution reveals two paths of force transmission through the kinetochore. *In preparation*.
- **Hamilton, G.E**., Dimitrova, Y.N., and Davis, T.N. Seeing is believing: our evolving view of kinetochore, structure, function, and assembly. Current Opinion in Cell Biology. Volume 60, October 2019, pages 44-52.
- Austin, R.N., Born, D., Lawton, T.J., and **Hamilton, G.E**. Protocols for purifying and characterizing integral membrane AlkB enzymes. Hydrocarbon and Lipid Microbiology Protocols, 2015.

PRESENTATIONS AT PROFESSIONAL MEETINGS

- Student ePoster presented at AAAS 2020 (February 2020)
- Co-led a workshop entitled “Navigating Difficult Situations in Science Communication” at Science Talk 2019 (April 2019)
- Guest lecture on biophysical techniques at South Seattle Community College (March 2019)
- Poster presented at EMBO Workshop: Chromosome Segregation and Aneuploidy (May 2019)
- Poster presented at Gordon Research Seminar on Centromere Biology (July 2018)

SCIENCE COMMUNICATION AND OUTREACH

- Creator and host of “Phosphorus,” a biochemistry podcast
- Science correspondent for Town Hall Seattle
- Presented a UW Science Now lecture to the public (April 2018)

GRANTS AND AWARDS

- National Institute of Health Molecular Biophysics Training Grant (2017-2019).
- UW School of Medicine Hurd Fellowship in Biophysics (2016-2017).
- National Science Foundation Graduate Research Fellowship Program Honorable Mention (2016)